UCRL-17631
cy. 2

University of California

Ernest O. Lawrence Radiation Laboratory

PROPERTIES OF THE Ξ^- AND THE Ξ^* (1817) FROM K^-p INTERACTIONS ABOVE 1.7 BeV/c

Deane W. Merrill and Janice Button-Shafer

July 10, 1967

RECEIVED
LAWRENCE
RADIATION LABORATORY

LIBR
DOCUME

TWO-WEEK LOAN COPY

This is a Library Circulating Copy which may be borrowed for two weeks. For a personal retention copy, call Tech. Info. Division, Ext. 5545

UCRL-17631
Cy. 2

E-1 R-

DISCLAIMER

This document was prepared as an account of work sponsored by the United States Government. While this document is believed to contain correct information, neither the United States Government nor any agency thereof, nor the Regents of the University of California, nor any of their employees, makes any warranty, express or implied, or assumes any legal responsibility for the accuracy, completeness, or usefulness of any information, apparatus, product, or process disclosed, or represents that its use would not infringe privately owned rights. Reference herein to any specific commercial product, process, or service by its trade name, trademark, manufacturer, or otherwise, does not necessarily constitute or imply its endorsement, recommendation, or favoring by the United States Government or any agency thereof, or the Regents of the University of California. The views and opinions of authors expressed herein do not necessarily state or reflect those of the United States Government or any agency thereof or the Regents of the University of California.

Submitted to the Physical Review

UCRL-17631
Preprint

UNIVERSITY OF CALIFORNIA
Lawrence Radiation Laboratory
Berkeley, California

AEC Contract No. W-7405-eng-48

PROPERTIES OF THE Ξ^- AND THE Ξ^* (1817) FROM K^-p INTERACTIONS ABOVE 1.7 BeV/c

Deane W. Merrill and Janice Button-Shafer

July 10, 1967

Properties of the Ξ^- and the $\Xi^*(1817)$ from K^-p Interactions above 1.7 BeV/c*

Deane W. Merrill† and Janice Button-Shafer‡

Lawrence Radiation Laboratory
University of California
Berkeley, California

July 10, 1967

ABSTRACT

A sample of 2529 Ξ^- hyperons, produced in Ξ^-K^+, $\Xi^-K^{\overset{+}{o}}\pi^{\overset{o}{+}}$, and $\Xi^-K^{\overset{+}{o}}\pi^{\bar{o}}\pi^+$ final states by K^- (in hydrogen) at incident momenta from 1.7 to 2.7 BeV/c, has been analyzed. The data are from an exposure of 26 events/ μb ("K-63" run) in the Alvarez 72-inch bubble chamber; approximately 85% of the Ξ^- events with visible Λ decay have been analyzed. A maximum-likelihood fit (with $\alpha_\Lambda = 0.656 \pm 0.055$ and with the Ξ spin = 1/2) yields the following values of Ξ^- decay parameters: $\alpha_{\Xi^-} = -0.375 \pm 0.051$; $\Phi_{\Xi^-} \equiv \tan^{-1}(\beta_{\Xi^-}/\gamma_{\Xi^-}) = 9.8^o \pm 11.6^o$. Our Spin analysis of the 3400 Ξ^- decays from the K-72 and K-63 experiments gives likelihood results which favor $J_\Xi = 1/2$ over $J_\Xi = 3/2$ by the equivalent of approximately 2.5 standard deviations. Analysis of the $\Xi^*(1817) \to \Xi^*(1530) + \pi$ decay mode indicates that the hypotheses $J^P = 1/2^+, 1/2^-, 3/2^-, 5/2^+, 7/2^-$, etc. are favored; but results are inconclusive because of high background as well as poor statistics. Analysis of the $\Xi^*(1817) \to \Lambda + \bar{K}$ provides no spin or parity discrimination. The K-63 beam channel is briefly described.

Properties of the Ξ^- and the $\Xi^*(1817)$ from K^-p Interactions above 1.7 BeV/c*

Deane W. Merrill† and Janice Button-Shafer‡

Lawrence Radiation Laboratory
University of California
Berkeley, California

July 10, 1967

I. INTRODUCTION

Prior to this experiment approximately 2600 Ξ^- had been analyzed to determine the Ξ^- decay parameters α_{Ξ^-} and $\Phi_{\Xi^-} \equiv \tan^{-1}(\beta_{\Xi^-}/\gamma_{\Xi^-})$.[1-6] The largest single sample previously analyzed consisted of 1004 events from the K-72 experiment[1] (K^-p at 1.2-1.7 GeV/c), for which the values $\alpha_{\Xi^-} = -0.368 \pm 0.057$ and $\Phi_{\Xi^-} = 0.5^\circ \pm 10.7^\circ$ (with $\alpha_\Lambda = 0.641 \pm 0.056$ and with the Ξ spin assumed to be 1/2) were reported. In this paper we describe the analysis of 2529 Ξ^- events in the K-63 experiment (K^-p at 1.7-2.7 GeV/c), including 224 Ξ^-K^+ events previously analyzed.[6,7] From K-63 data we obtain values $\alpha_{\Xi^-} = -0.375 \pm 0.051$ and $\Phi_{\Xi^-} = 9.8^\circ \pm 11.6^\circ$ (with $J_{\Xi^-} = 1/2$ and $\alpha_\Lambda = 0.656 \pm 0.055$), in good agreement with previously reported values. Combining our data with 902 K-72 events, we obtain (with $\alpha_\Lambda = 0.657 \pm 0.047$) $\alpha_{\Xi^-} = -0.394 \pm 0.041$ and $\Phi_{\Xi^-} = 9.9 \pm 9.0^\circ$.

The Ξ spin is also analyzed in a combined sample which includes 900 Ξ^- and 150 Ξ^0 events from the K-72 experiment.[1,8]

The decay properties of the $\Xi^*(1530)$ and the $\Xi^*(1817)$ have been analyzed in earlier published work.[9-11] In these areas we have treated a somewhat larger data sample, but no essential modification of earlier results is indicated.

A later paper will treat other topics, such as Ξ^0 decay parameters and production systematics.

II. DESCRIPTION OF THE K-63 BEAM CHANNEL

The data analyzed in this report were obtained from photographs of K^-+p interactions in the Laboratory's 72-inch bubble chamber. Most of the data are from a 1.7 to 2.7 BeV/c separated K^- beam (K-63) designed by Joseph J. Murray with the assistance of J. Button-Shafer; however, our analysis of Ξ^- decay properties includes data from an earlier beam, K-72 (designed by Harold K. Ticho and others).[12]

Figures II-1 and II-2 illustrate the general features of the K-63 beam, which has been described in detail elsewhere.[13,14] The Bevatron internal proton beam (operating at 6.1 BeV, 1.2×10^{12} protons/pulse) strikes a copper target 4 in. long by 1/8 in. wide by 1/16 in. high. The secondary beam channel accepts $\approx$ 0.10 msr at an angle of 0°. Momentum selection ($\approx \pm$ 1.5% about the nominal momentum) is performed by collimators at mass slit 1, after horizontal dispersion in M3. Electrostatic separators S1 and S2 separate K^- from background (mostly π^-) in two stages, in the vertical plane. These separators, of the glass-cathode type described in Ref. 15, maintain a potential of 500 kV across a 2-inch gap. At the two mass slits, K^- and π^- are focused into images 1/16 in. high separated by $\approx$ 1/8 in. The K^- pass through the slits to the bubble chamber, whereas the π^-, passing through uranium in the slit jaws (see Fig. II-3), lose $\gtrsim$ 8% of their momentum and are swept aside by the bending magnet M4.

The rather broad momentum bite necessitated the use of special cocked mass slits, a design feature utilized for perhaps the first time in a bubble-chamber beam. One of these slits (#1) is described in Fig. II-3; slit #2 is similar in design but more nearly parallel to the beam direction. Particles are focused at various distances (y) along the beam axis, the higher-momentum particles being focused further downstream. The bending in the Bevatron field and in magnet M3 produces horizontal dispersion; and the mass slit is designed so that a particle of any momentum (in the 3% interval) is focused at some point along the mass slit. Images in the horizontal and vertical planes approximately coincide and "track" linearly with momentum to follow the mass slit. (Degrading and multiple scattering in the tapered jaws were studied by computer calculations; uranium was found more effective in eliminating pions than iron or copper.)

The critical design requirements necessitated the use of many quadrupoles, which were carefully corrected for aberrations.[16] Optimum quadrupole positions and currents were calculated with a special analog computer designed by Murray.[14] The beam was tuned for initial running in July, 1963.

Over an 18-month period, 2376 rolls (average $\approx$ 630 frames/roll) of K^- film were photographed, including: (a) 897 rolls at 2.45 to 2.7 BeV/c; (b) 235 rolls at

2.1 BeV/c; (c) 249 rolls at 1.7 BeV/c;[17] (d) 26 rolls at 2.9 BeV/c, which had unacceptably low K^- yield and high background; (e) 321 rolls at 2.0 BeV/c, for UCLA; (f) 425 rolls at 2.1 BeV/c, with lead plates in the chamber; and (g) 223 rolls in D_2 (no lead plates), at 2.1 and 2.63 BeV/c. Only the data from (a), (b), and (c), amounting to $\approx$ 26 events/μbarn, are discussed in this report; in this exposure, we observe 6 to 10 beam tracks per frame, including 15 to 35% non-K^- background.

The same beam setup was used for a π^- exposure from 1.6 to 4.2 BeV/c.

III. SELECTION OF Ξ EVENTS

After being topologically scanned, the events of the K-63 experiment were measured either on one of the Franckenstein measuring projectors or on one of the SMP's (scanning and measuring projectors).[18] The measured events were processed on the IBM 7094 or 7044 with the standard data-analysis programs of the Alvarez group--PANAL, PACKAGE, WRING, AFREET, and DST-EXAM. Failing events (events failing to fit acceptably any kinematic hypothesis) were remeasured and, when necessary, re-examined at the scanning table. For ambiguous events, ionization information was used wherever possible to distinguish between competing hypotheses.

The actual fitting of the events, done by PACKAGE, begins with a three-dimensional reconstruction of each measured track; appropriate corrections are made for energy loss, optical distortions, and non-uniformity of the magnetic field.[19] The measured momenta and angles of each track at a production or decay vertex are adjusted to give a best fit to each of several particle-assignment hypotheses, and a χ^2 is calculated. In DST-EXAM the χ^2 values from individual vertices are combined to form an overall confidence level for each of several production and decay hypotheses, on the basis of which the most likely hypothesis is selected. Events passing no hypothesis with a confidence level ≥ 0.005 are not used.

In this paper we consider only Ξ^- events in which both the Ξ^- and Λ decay visibly in the chamber; these occur in the following final states and topologies:

Event-type 72 (vee with two prongs and negative decay vertex):

$$\begin{aligned} K^- + p &\rightarrow \Xi^- + K^+ \\ &\rightarrow \Xi^- + K^+ + \pi^0 \\ &\rightarrow \Xi^- + K^0 + \pi^+ \ (K^0 \text{ unseen}) \\ &\rightarrow \Xi^- + K^+ + \text{neutrals} \\ &\rightarrow \Xi^- + \pi^+ + \text{neutrals}, \end{aligned} \tag{1}$$

Event-type 74 (vee with four prongs and negative decay vertex):

$$K^- + p \rightarrow \Xi^- + K^+ + \pi^+ + \pi^- , \tag{2}$$

Event-type 12 (two vees, two prongs, and negative decay vertex):

$$\begin{aligned} K^- + p &\rightarrow \Xi^- + K^0 + \pi^+; \quad K^0 \rightarrow \pi^+ + \pi^- \ (K^0 \text{ seen}) \\ &\rightarrow \Xi^- + K^0 + \pi^+ + \pi^0; \ K^0 \rightarrow \pi^+ + \pi^- \ (K^0 \text{ seen}). \end{aligned} \tag{3}$$

In fitting each of the hypotheses, we made a 3C (three-constraint) fit at the Λ decay vertex, and a 3C fit at the K^0 decay vertex where a K^0 was observed. The fitted Λ momentum was used in a 4C fit (3C for events having short Ξ^-) at the Ξ^- decay vertex. Finally the fitted Ξ^- momentum was used in a 4C fit, a 1C fit, or a missing-mass calculation at the production vertex.

In Table III-1 we list, according to topology and final state, the number of events obtained at each

Table III-1. Final states and momenta of Ξ^- events analyzed.

		Ξ^- event type							
		72					12		74
Expt.	p (BeV/c)	Ξ^-K^+	$\Xi^-K^+\pi^0$	$\Xi^-K^0\pi^+$	Ξ^-K^+ +neutrals	$\Xi^-\pi^+$ +neutrals	$\Xi^-K^0\pi^+$	$\Xi^-K^0\pi^+\pi^0$	$\Xi^-K^+\pi^+\pi^-$
K-63	1.7	272	31	54	0	0	0	0	0
K-63	2.1	342	105	173	1	6	94	0	4
K-63	2.45	76	47	50	6	7	24	10	8
K-63	2.55	103	66	85	15	24	26	6	17
K-63	2.6	153	131	145	28	45	67	15	38
K-63	2.7	76	49	54	13	24	22	6	11
K-63 total		**1022**	**429**	**561**	**63**	**106**	**233**	**37**	**78**

momentum in the K-63 experiment. The events listed represent approximately 85% of the events that will eventually be available when the remeasurement process has been completed.

The identification of a Ξ^- with visible Λ decay, even without ionization information, is completely unambiguous. Of the 2181 type-72 events listed, not one was ambiguous with the other hypotheses tested, namely:

$$\begin{aligned} K^-+p &\rightarrow \Xi^-+K^0+\pi^+;\ \Xi^- \rightarrow \Lambda+\pi^-;\ K^0 \rightarrow \pi^++\pi^- \\ &\rightarrow \Xi^-+K^0+\pi^++\pi^0;\ \Xi^- \rightarrow \Lambda+\pi^-;\ K^0 \rightarrow \pi^++\pi^- \\ &\rightarrow \Sigma^-+K^++K^0;\ \Sigma^- \rightarrow n+\pi^-;\ K^0 \rightarrow \pi^++\pi^- \end{aligned} \quad (4)$$

No competing hypotheses were tested for event type 74 or 12.

About 6% of the events listed are ambiguous between two or more hypotheses; the ambiguities involving $\Xi^-K^+\pi^0$ and $\Xi^-K^0\pi^+$ final states (in event type 72) are most numerous. Our analysis of Ξ^- decay parameters, however, is virtually independent of the final state in which the Ξ^- is produced, so that we retain in our sample events ambiguous between two or more final states involving Ξ^- with visible Λ decay.[20]

Table III-2 lists the subsamples into which the data were divided for analysis. The older K-72 experiment is included.

For more detailed discussion of the selection of events, especially the separation of π^--p from K^--p interactions, see Ref. 21.

Table III 2. Subsamples used in Σ decay parameter analysis.

Subsample						
Expt.	Final state	p(BeV/c)	Events	Sub-samples	Events per subsample	$\hat{\Xi}\cdot\hat{K}$ cutoff points
K-63	Ξ^-K^+	1.7	272	4	68	0.88, 0.70, -0.07
K-63	Ξ^-K^+	2.1	342	5	68	0.90, 0.75, 0.45, -0.43
K-63	Ξ^-K^+	2.45, 2.55	179	2	89	0.73
K-63	Ξ^-K^+	2.6 , 2.7	229	3	76	0.89, 0.50
K-63	$\Xi^-K^+\pi^0$	1.7 , 2.1	136	2	68	0.43
K-63	$\Xi^-K^+\pi^0$	2.45, 2.55	113	2	56	a
K-63	$\Xi^-K^+\pi^0$	2.6 , 2.7	180	2	90	0.43
K-63	$\Xi^-K^0\pi^+$	1.7 , 2.1	321	4	80	0.58, 0.20, -0.36
K-63	$\Xi^-K^0\pi^+$	2.45, 2.55	185	3	62	0.70, 0.07
K-63	$\Xi^-K^0\pi^+$	2.6 , 2.7	288	4	72	0.78, 0.43, -0.17
K-63	$\Xi^-K\pi\pi$	All	115	1	115	--
K-63	Ξ^-K^++neutrals	All	169	2	85	0.04
K-63	$\Xi^-\pi^+$+neutrals	All				
K-63	Total		2529	34	75	--
K-72	Ξ^-K^+	1.2-1.4	194	3	65	0.69, 0.10
K-72	Ξ^-K^+	1.5	470	7	67	0.90, 0.78, 0.59 0.29, -0.13, -0.53
K-72	Ξ^-K^+	1.6, 1.7	166	2	83	0.66
K-72	$\Xi^-K^0\pi^+$	All	72	1	72	--
K-72	Total		902	13	69	--

[a]Both subsamples contain events from $\hat{\Xi}\cdot\hat{K}$ = - 1 to +1.

IV. THEORY

In this paper we shall discuss the decay properties of the Ξ hyperon and the $\Xi^*(1817)$. The Ξ decays weakly, principally via the non-leptonic modes

$$\Xi^- \to \Lambda + \pi^- \qquad (5)$$
$$\Xi^0 \to \Lambda + \pi^0 \quad .$$

The $\Xi^*(1817)$ decays strongly, principally via [9, 10, 22-25]

$$\Xi^*(1817) \to \Lambda + \bar{K} \qquad (6)$$
$$\Xi^*(1817) \to \Xi^*(1530) + \pi \quad .$$

We may schematically represent these processes by

$$F_J \to F_{J'} + B_0 \quad , \qquad (7)$$

where F_J, $F_{J'}$, and B_0 are a fermion of spin J, a fermion of spin J', and a spinless boson, respectively. The angular distributions in a decay process of this type have been investigated by a number of authors, including Capps,[26] Gatto and Stapp,[27] Byers and Fenster,[28] Ademollo and Gatto,[29] Button-Shafer,[30] Zemach,[31] and Berman and Jacob.[32] We shall lean most heavily on the work of Byers and Fenster (cast into a maximum-likelihood framework);[33] this uses the language of irreducible tensors T_{LM} for the special case J' = 1/2. We shall also use Ref. ~~ence~~ 30, an extension of the Byers-Fenster formalism, to treat the case J' = 3/2.

The Byers-Fenster type of formalism has several appealing features: (i) the initial spin state of F_J is described

by a complete set of independent parameters, without assumptions regarding the mechanisms that produced F_J; (ii) the mechanism describing the decay of F_J may be described in terms of simple helicity amplitudes; (iii) the spin state of F_J, is expressed in terms of expectation values of a complete set of orthogonal spin operators. As a result, one can readily formulate tests to extract all possible information (about the spin and decay properties of F_J) from a given set of observed decays.

Coordinate Systems and Relativistic Transformations

Figure IV-1 illustrates Ξ production and decay via the sequence (A) $K^- + p \rightarrow \Xi + K$; (B) $\Xi \rightarrow \Lambda + \pi$; (C) $\Lambda \rightarrow p + \pi$. In the c.m. frame (A), the axes X,Y,Z, and the Ξ production angle Θ are defined in terms of the incoming K^- direction $\hat{K}$ and the outgoing Ξ direction $\hat{\Xi}$. In the Ξ rest frame (B), the Λ direction $\hat{\Lambda}$ is defined in terms of angles θ and ϕ. In the rest frame (C), the Λ polarization $\vec{P}_\Lambda$ and the proton direction $\hat{p}$ are described with reference to axes x and y, illustrated in the expanded view (upper left) of system (B).

In a particle's own rest frame, its spin state and the angular distribution of its decay products, are conveniently expressed in terms of tensors formed from the three components of a spin operator $\vec{S}$. When one wishes to describe multistep production and decay processes

similar to that of Fig. IV-1, the three-dimensional description of spin states may be used (even in the relativistic region), provided the observed momenta of the reaction are transformed successively through all intermediate rest frames, via successive "direct Lorentz transformations."[34, 35]

Description of Initial Spin State

Using the language of Byers and Fenster,[28] we expand the initial-state density matrix ρ_i[36] in terms of irreducible tensor operators T_{LM}:

$$(\rho_i)_{jk} = \frac{1}{2J+1} \sum_{L=0}^{2J} \sum_{M=-L}^{L} (2L+1)\, t^*_{LM} (T_{LM})_{jk} , \qquad (8)$$

where the quantities $t_{LM} = \mathrm{Tr}(\rho_i T_{LM})$ are expectation values of the T_{LM}. The T_{LM} are normalized so that close in

$$\mathrm{Tr}(T_{L'M'} T^{\dagger}_{LM}) = \frac{2J+1}{2L+1} \delta_{LL'} \delta_{MM'} , \qquad (9)$$

and are formed from spin operators S_x, S_y, and S_z, as the spherical harmonics Y_{LM} are formed from coordinates x,y, and z. [For example, $T_{11} \propto (S_x + iS_y)$, in analogy with $Y_{11} \propto (x + iy)$.] The tensor operators T_{LM} and the expectation values t_{LM} obey the relations

$$\left(\begin{array}{l} T_{L,-M} = (-)^M T^{\dagger}_{LM} \\ \\ t_{L,-M} = (-)^M t^*_{LM} \end{array} \right) . \qquad (10)$$

close up

Hence t_{L0} is real. The normalization condition $Tr\,\rho_i = 1$ implies that $t_{00} = 1$. The matrix representation of the T_{LM} depends upon the dimensionality (2J+1) of the spin space, and also upon the choice of basis vectors used to define the space. In a representation where T_{L0} is diagonal, the matrix elements of the T_{LM} are real, and equal to Clebsch-Gordan coefficients:

$$\left(T_{LM}\right)_{M''M'} = C(JLJ;\, M'M)\,\delta_{M'',\,M'+M} \tag{11}$$

$$= (-)^{J-M'}\left(\frac{2J+1}{2L+1}\right)^{1/2} C(JJL;M'',-M')\,\delta_{M,M''-M'}\,.$$

(The notation for the Clebsch-Gordan coefficients corresponds to $C(j_1j_2j_3;\, m_1m_2)$, where $\vec{j}_1 + \vec{j}_2 = \vec{j}_3$ and $m_1 + m_2 = m_3$.)

Noting that t_{10} is related to the expectation value of the spin operator S_z by

$$t_{10} = \left[\frac{1}{J(J+1)}\right]^{1/2} \langle S_z \rangle\,, \tag{12}$$

one obtains an upper limit for $|t_{10}|$, for any spin J:

$$|t_{10}| \leqslant \left(\frac{J}{J+1}\right)^{1/2}. \tag{13}$$

Similar relations may be derived for other t_{LM}. An additional restriction on the permitted range of the t_{L0} is imposed by the requirement that the diagonal elements of the density matrix be real and non-negative. Substituting appropriate values of the matrix elements $\left(T_{LM}\right)_{jk}$ into Eq. (8), one obtains the following

inequalities:

For J = 1/2:

$$1 \pm \sqrt{3}\, t_{10} \geqslant 0 \,. \tag{14}$$

For J = 3/2:

$$\begin{aligned} &1 \pm 3\sqrt{\tfrac{3}{5}}\, t_{10} + \sqrt{5}\, t_{20} \pm \sqrt{\tfrac{7}{5}}\, t_{30} \geqslant 0 \\ &1 \pm \sqrt{\tfrac{3}{5}}\, t_{10} - \sqrt{5}\, t_{20} \mp 3\sqrt{\tfrac{7}{5}}\, t_{30} \geqslant 0 \,. \end{aligned} \tag{15}$$

#

For J = 5/2:

$$1 \pm 3\sqrt{\tfrac{5}{7}}\, t_{10} + 5\sqrt{\tfrac{5}{14}}\, t_{20} \pm \sqrt{\tfrac{35}{6}}\, t_{30} + 3\sqrt{\tfrac{3}{14}}\, t_{40} \pm \sqrt{\tfrac{11}{42}}\, t_{50} > 0$$

$$1 \pm 9\sqrt{\tfrac{1}{35}}\, t_{10} - \sqrt{\tfrac{5}{14}}\, t_{20} \mp 7\sqrt{\tfrac{7}{30}}\, t_{30} - 9\sqrt{\tfrac{3}{14}}\, t_{40} \mp 5\sqrt{\tfrac{11}{42}}\, t_{50} > 0$$

$$1 \pm 3\sqrt{\tfrac{1}{35}}\, t_{10} - 2\sqrt{\tfrac{10}{7}}\, t_{20} \mp 2\sqrt{\tfrac{14}{15}}\, t_{30} + 3\sqrt{\tfrac{6}{7}}\, t_{40} \pm 5\sqrt{\tfrac{22}{21}}\, t_{50} > 0 \,.$$

If all t_{L0} having L > 1 are zero, these various inequalities reduce to the condition

$$|t_{10}| \leqslant \frac{1}{3}\sqrt{\frac{J+1}{J}} \,. \tag{17}$$

The inequalities (13) and (17) are equivalent to the two inequalities of Lee and Yang:[37]

$$|\langle \cos\theta \rangle| \equiv |\langle \hat{F}_J \cdot \hat{n} \rangle| \leqslant \frac{1}{2J+2} \tag{18}$$

lower

and

$$|\langle \cos\theta \rangle| \leqslant \frac{1}{6J} \,. \tag{19}$$

Equation (19) holds only if no powers higher than (cos θ) appear in the F_J decay distribution $I(\theta,\phi)$.

Further inequalities restricting the values of the t_{LM} have been pointed out by Byers and Fenster,[28] and others,[38] but in our analysis these inequalities provide no new information.

In certain cases some of the t_{LM} may vanish due to symmetries in the production process. For example, for particles J produced in a parity-conserving reaction of the type

$$A + B \xrightarrow{\#} J + C + D + E + \ldots , \qquad (20)$$

the expectation values t_{LM} describing the spin state of the particles J in their rest frame vanish for odd M, provided:

(i) the axis of quantization of the t_{LM} is the production normal

$\hat{z} = \hat{A} \times \hat{J}$;

(ii) the beam and target particles (A and B) are unpolarized, and averages are taken over the spin states of the final-state particles C,D,E, etc.;

(iii) averages are taken over all directions of C,D,E, etc.

(This is a generalization of Capps' Checkerboard Theorem.[26])

Because of the symmetries in the production reaction, we choose to express the initial-state density matrix ρ_i in the (X,Y,Z) coordinate system, having as its Z-axis

the production normal $\hat{n}$. (See Fig. IV-1.) Hence M must consist of two parts: a rotation matrix $R(\phi,\theta,0)$ transforming ρ_i into the helicity representation,[39] and the diagonalized transition matrix M' describing the actual decay. That is,

$$\rho_f = M' R(\phi,\theta,0)\ \rho_i\ R^{\dagger}(\phi,\theta,0)\ (M')^{\dagger} \tag{21}$$

where M' and ρ_f are represented in the helicity system (x,y,z) and ρ_i in the production system (X,Y,Z).

The element of the complete decay matrix $M \equiv M' R\ (\phi,\theta,0)$ may be written[40]

$$(M)_{\lambda m} = A_\lambda [(2J+1)/4\pi]^{1/2} \mathcal{D}^{J^*}_{m\lambda}(\phi,\theta,0), \tag{22}$$

where λ is the projection of spin J (and J') on the helicity z-axis, and m is the projection of spin J on the production Z-axis. The "helicity amplitudes" A_λ are the elements of the diagonalized transition matrix M', each representing the probability amplitude for the process (with helicity λ).

$$|J,\lambda\rangle \rightarrow |J',\lambda\rangle + B_0\ . \tag{23}$$

$\mathcal{D}^J_{m_1 m_2}$

The functions $\mathcal{D}^J_{m_1 m_2}(\alpha,\beta,\gamma)$ are the usual matrix elements of the rotation operator $R(\alpha,\beta,\gamma)$: $\mathcal{D}^J_{m_1 m_2}(\alpha,\beta,\gamma) =$ $\exp(-m_1\alpha)\ d^J_{m_1 m_2}(\beta)\ \exp(-im_2\gamma)$. (See, for example, Jacob and Wick.[41]) #

i

In general, the decay process $F_J \rightarrow F_{J'} + B_0$ can proceed via several different partial waves ℓ, where ℓ may assume values from $|J-J'|$ to $|J+J'|$. In strong decay,

only those partial waves consistent with parity conservation contribute to the decay amplitude. In terms of the usual complex partial-wave decay amplitudes a_ℓ, the helicity amplitudes of Eq. (22) have the form [40]

$$A_\lambda = (-)^{\lambda-J'} \sum_\ell a_\ell \; C(JJ'\ell;\lambda,-\lambda) \quad . \tag{24}$$

Byers and Fenster[28] (and Button-Shafer[30]) simplify the expression for ρ_f by utilizing the orthogonality properties of the $\mathcal{D}^J_{M\lambda}$ functions and Clebsch-Gordan coefficients. The general form (in the helicity representation) is [40]

$$\begin{aligned}(\rho_f)_{\lambda\lambda'} &\equiv \langle J',\lambda|\rho_f|\,J',\lambda'\rangle = (-)^{J-\lambda'}(A_\lambda A^*_{\lambda'}/4\pi)\,(2J+1)^{1/2} \\ &\times \sum_{L=0}^{2J} \sum_{M=-L}^{L} \left[(2L+1)^{1/2}\, C(JJL;\lambda,-\lambda')\, t^*_{LM}\, \mathcal{D}^{L^*}_{M,\lambda-\lambda'}(\phi,\theta,0)\right],\end{aligned} \tag{25}$$

which is valid for any spin J and J' (integer as well as half-integer). We note that only the $\mathcal{D}^{L^*}_{M,\lambda-\lambda'}(\phi,\theta,0)$ having <u>integral</u> indices L,M, and $(\lambda-\lambda')$ appear in Eq. (25) and that each t_{LM} describing the initial F_J multiplies a single $\mathcal{D}^{L^*}_{M,\lambda-\lambda'}$ function.

Having arrived at an expression for the final-state density matrix, one may calculate the angular distribution of the decay process

$F_J \to F_J' + B_0$ as

$$I(\theta,\phi) = \mathrm{Tr}(\rho_f) \quad . \tag{26}$$

A complete description of the spin state of F_J' as a function of θ and ϕ is obtained by calculating the quantities (with T_{LM} operators now used in the F_J' spin space, helicity representation)

$$I \langle T_{LM} \rangle (\theta,\phi) = \mathrm{Tr}\,(\rho_f T_{LM}) \quad . \tag{27}$$

With slight deviation from the work of Byers and Fenster, we now evaluate (26) and (27) for the special case $J' = 1/2$. Then we discuss some of the results obtained by Button-Shafer for the special case of strong decay with $J' = 3/2$.

a. <u>Spin J →spin 1/2 + spin 0.</u>

For weak decay, the two partial waves $a \equiv a_{J-\frac{1}{2}}$ and $b \equiv a_{J+\frac{1}{2}}$ can contribute to the transition matrix M. One customarily defines

$$\begin{aligned} \alpha + i\,\beta &\equiv (\mathrm{Re} + i\,\mathrm{Im})[a^* b/(|a|^2 + |b|^2)] \\ \gamma &\equiv (|a|^2 - |b|^2)/(|a|^2 + |b|^2) \end{aligned} \tag{28}$$

so that $\alpha^2 + \beta^2 + \gamma^2 = 1$. Alternatively, the parameters β and γ may be expressed in terms of independent parameters a and Φ:

$$\beta + i\,\gamma \equiv [1 - \alpha^2]^{1/2} e^{i\Phi} \quad . \tag{29}$$

Using Eqs. (26) and (27) with T_{LM} proportional to σ_z and $\sigma_x + i\sigma_y$ (L,M = 1,0 and 1,1) one arrives at the result[6, 28, 33]

$$I(\theta,\phi) = \left[\sum_{\substack{L=0 \\ L \text{ even}}}^{2J-1} + \alpha \sum_{\substack{L=1 \\ L \text{ odd}}}^{2J} \right] \sum_{M=-L}^{L} n^J_{L0}\, t_{LM}\, Y^*_{LM}(\theta,\phi) \qquad (30a)$$

$$\underset{\sim}{I\vec{P}} \cdot \hat{z} = \left[\alpha \sum_{\substack{L=0 \\ L \text{ even}}}^{2J-1} + \sum_{\substack{L=1 \\ L \text{ odd}}}^{2J} \right] \sum_{M=-L}^{L} n^J_{L0}\, t_{LM}\, Y^*_{LM}(\theta,\phi) \qquad (30b)$$

#

$$\underset{\sim}{I\vec{P}} \cdot \hat{x} + i\, \underset{\sim}{I\vec{P}} \cdot \hat{y} = (-\gamma + i\beta)(2J+1) \sum_{\substack{L=1 \\ L \text{ odd}}}^{2J} \sum_{M=-L}^{L} n^J_{L0}\, t_{LM}\, \mathcal{O}^L_{M1}(\phi,\theta,0)$$

$$(30c)$$

times

$$\times [(2L+1)/4\pi]^{1/2}\, [L(L+1)]^{-1/2} ,$$

where

$$n^J_{L0} \equiv (-)^{J-\frac{1}{2}}\, [(2J+1)/4\pi]^{1/2}\, C(JJL;\tfrac{1}{2},-\tfrac{1}{2}) \qquad (31)$$

For the two-step decay process

$$\Xi \to \Lambda + \pi;\ \Lambda \to p + \pi , \qquad (32)$$

the joint angular distribution of the Λ (in the Ξ rest frame) and of the decay proton (in the Λ rest frame) is given by

$$I(\hat{\Lambda},\hat{p}) \propto I(\hat{\Lambda})\, [1 + \alpha_\Lambda \underset{\sim}{\vec{P}_\Lambda}(\hat{\Lambda}) \cdot \hat{p}]$$

$$= I(\theta,\phi) + \alpha_\Lambda [\underset{\sim}{I\vec{P}_\Lambda} \cdot \hat{\Lambda}(\hat{p}\cdot\hat{\Lambda}) + \underset{\sim}{I\vec{P}_\Lambda} \cdot \hat{x}(\hat{p}\cdot\hat{x}) + \underset{\sim}{I\vec{P}_\Lambda} \cdot \hat{y}(\hat{p}\cdot\hat{y})], \qquad (33)$$

# # #

where the Λ angular distribution $I(\theta,\phi)$ and the Λ polarization components $I\vec{P}_\Lambda\cdot\hat{x}$, $I\vec{P}_\Lambda\cdot\hat{y}$, and $I\vec{P}_\Lambda\cdot\hat{z} \equiv I\vec{P}_\Lambda\cdot\hat{\Lambda}$ are given by Eqs. (30) . #

The distribution in $(\hat{p}\cdot\hat{\Lambda})$ is obtained by integrating Eq. (33) over θ,ϕ, and $\phi_p \equiv \tan^{-1}[(\hat{p}\cdot\hat{y})/(\hat{p}\cdot\hat{x})]$:

$$\mathcal{L}(\hat{p}.\hat{\Lambda}) \propto 1 + \alpha_\Lambda\,\alpha_\Xi\,(\hat{p}\cdot\hat{\Lambda}); \tag{34}$$

This relation holds for any spin J. Thus a spin-independent estimate of α_Ξ is possible even if all t_{LM} with $L > 0$ are zero.

The presence of non-zero t_{LM} with $L > 0$ permits a more accurate (and spin-dependent) determination of α_Ξ. If the Ξ has spin 1/2 and polarization $P_\Xi \equiv \vec{P}_\Xi\cdot\hat{n} = \sqrt{3}\,t_{10}$, the distribution function (33) reduces to the familiar form

$$I(\hat{\Lambda},\hat{p}) \propto 1 + \alpha_\Xi P_\Xi \cos\theta + \alpha_\Lambda\,(\hat{p}\cdot\hat{\Lambda})\,[\alpha_\Xi + P_\Xi\cos\theta] + \alpha_\Lambda P_\Xi \sin\theta\,[\beta_\Xi\hat{p}.\hat{y} - \gamma_\Xi\hat{p}\cdot\hat{x}]\,. \tag{35}$$

For either strong or weak decay, three features of the decay distribution enable one, in principle, to determine the spin J: (i) a lower limit for J is established by the maximum complexity of the observed distribution; i.e., $J \geqslant L_{max}/2$ where L_{max} is the L-value of the highest non-zero t_{LM}; (ii) if $|t_{10}|$ or any other $|t_{LM}|$ exceeds its J-dependent bounds, an upper limit for

The above equations hold also for a decay such as $\Xi^*(1817) \to \Lambda + \bar{K}$; $\Lambda \to p + \pi^-$ if α_{Ξ^*} and β_{Ξ^*} are set equal to zero and γ_{Ξ^*} taken as ± 1.

J may be established by inequalities similar to the Lee-Yang inequalities (18) and (19); (iii) if any odd-L t_{LM} are non-zero, a best value of the factor (2J+1) of Eq. (30c) may be determined experimentally.

For further discussion of the above formalism and use of the likelihood method see ~~Reference~~ Refs. 33, 6, or 21.

b. Strong decay: Spin J → spin 3/2 + spin 0.

The strong decay process

$$F_J \to F_{3/2} + B_0 \qquad (36)$$

(where $F_{3/2}$ is a spin-3/2 fermion) has been discussed by Button-Shafer,[30] Zemach,[31] and Berman and Jacob,[32] among others. We utilize the formalism of reference 30 which extends the Byers-Fenster theory to obtain a complete and general description of the decay process (36). All equations are discussed more extensively in Ref. 30, except for the introduction here of the parameter λ_0 (Eq. 48) and of the momentum-barrier treatment of higher ℓ-waves.

A variety of tests may be performed to determine the spin and parity of F_J; we shall describe here only those used in our analysis of the reaction

$$\Xi^*(1817) \to \Xi^*(1530) + \pi; \quad \Xi^*(1530) \to \Xi + \pi \ , \qquad (37)$$

(more space)

which we denote symbolically by

$$F_J \to F_{3/2} + B_0; \quad F_{3/2} \to F_{1/2} + B_0 \ . \qquad (38)$$

(more space)

The spin state of $F_{3/2}$ may be represented by a 4X4

times

density matrix ρ_f whose elements (in the helicity representation) are given by Eq. (25) . In particular, the diagonal elements are

$$(\rho_f)_{\lambda\lambda} = \sum_{L=0}^{2J} \sum_{M=-L}^{L} t^*_{LM} \, |A_\lambda|^2 \, n_{L0}^{(2\lambda)} Y_{LM}(\theta,\phi), \qquad (39)$$

where the t_{LM} describe the spin state of F_J, and where θ and ϕ define the direction of $F_{3/2}$ in the F_J rest frame. The helicity amplitudes A_λ are given by (24) , and the J-dependent constants $n_{L0}^{(2\lambda)}$ by the relation

$$n_{L0}^{(2\lambda)} = (-)^{J-\lambda}[(2J+1)/4\pi)]^{1/2} \, C(JJL;\, \lambda,-\lambda). \qquad (40)$$

The angular distribution of $F_{3/2}$ (in the F_J rest frame) is

$$\begin{aligned} I(\theta,\phi) &= \mathrm{Tr}\,(\rho_f) \\ &= 2 \sum_{\substack{L=0 \\ L \text{ even}}}^{2J-1} \sum_{M=-L}^{L} \left[|A_{3/2}|^2 n_{L0}^{(3)} + |A_{1/2}|^2 n_{L0}^{(1)} \right] t_{LM} Y_{LM}^*(\theta,\phi \end{aligned} \qquad (41)$$

A lower limit on the spin J is established by the maximum complexity of the observed $I(\theta,\phi)$ distribution; i.e., if the data require non-zero t_{LM} through order L, then $J \geq L/2$. No spin information is obtained from Eq. (41) if all t_{LM} having $L > 0$ are consistent with zero. One finds that $I(\theta,\phi)$ has a particularly simple form if ϕ is

ignored and only the lower ℓ-wave included, $1 + a_2 P_2 + a_4 P_4 \cdots$.[42]

If $F_{3/2}$ subsequently decays strongly via $F_{3/2} \to F_{1/2} + B_0$, the angular distribution of $F_{1/2}$ (in the $F_{3/2}$ rest frame) is given by the Byers-Fenster formalism:

$$\mathcal{L}(\psi) = \frac{1}{4\pi} I(\theta,\phi)\left[1 - \sqrt{5}\,\langle T_{20}\rangle(\theta,\phi)\, P_2(\cos\psi)\right], \qquad (42)$$

where ψ is the angle of $F_{1/2}$ relative to the $F_{3/2}$ direction of flight, ~~and~~ where ~~we have ignored~~ the azimuth of $F_{1/2}$ is ignored, and where $\langle T_{20}\rangle$ describes the $F_{3/2}$ spin state. The quantity

$$I\,\langle T_{20}\rangle(\theta,\phi) = \mathrm{Tr}\,(\rho_f T_{20})$$

$$= 2(5)^{-1/2} \sum_{\substack{L=0 \\ L\ \mathrm{even}}}^{2J-1} \sum_{M=-L}^{L} \left[|A_{3/2}|^2 n_{L0}^{(3)} - |A_{1/2}|^2 n_{L0}^{(1)}\right] t_{LM} Y^*_{LM}(\theta,\phi) \qquad (43)$$

represents the $\langle T_{20}\rangle$ component of $F_{3/2}$ "polarization" referred to helicity axes, i.e., the $F_{3/2}$ spin alignment along its direction of flight.

Combining Eqs. (41) through (43) and integrating over θ and ϕ (the angles describing the direction of $F_{3/2}$), we are left with only those terms containing t_{00}, so that[43]

$$\mathcal{L}(\psi) \propto 1 + b_2 P_2(\cos\psi) = 1 + b_2 (3\cos^2\psi - 1)/2\,, \qquad (44)$$

where

$$b_2 = (|A_{1/2}|^2 - |A_{3/2}|^2) \times (|A_{1/2}|^2 + |A_{3/2}|^2)^{-1}\,. \qquad (45)$$

(We have used the relation $n_{00}^{(1)} = n_{00}^{(3)}$.) After integration over θ and ϕ, the <u>azimuthal</u> distribution of

$F_{1/2}$ about the $F_{3/2}$ line of flight is isotropic.

If $J = 1/2$, then $A_{3/2} = 0$, so that $\mathfrak{b}_2 = 1.0$ regardless of the parity of J. If $J \geqslant 3/2$. the helicity amplitudes A_λ have the following form for various $\Xi^*(1817)$ spin and parity assumptions J^P [where P is the parity of $\Xi^*(1817)$ relative to that of $\Xi^*(1530)$]:

$J^P = 3/2^-, 5/2^+, 7/2^-$, etc.:

(Editor: Possible to set up as $\frac{3}{2}$?)

$$A_{1/2} \propto a(3J-3/2)^{1/2} - c(J+3/2)^{1/2} \qquad (46a)$$

$$A_{3/2} \propto a(J+3/2)^{1/2} + c(3J-3/2)^{1/2} \qquad (46b)$$

$J^P = 3/2^+, 5/2^-, 7/2^+$, etc.:

(set as $\frac{9}{2}$?)

$$A_{1/2} \propto b(J - 1/2)^{1/2} - d(3J+9/2)^{1/2} \qquad (47a)$$

$$A_{3/2} \propto b(3J+9/2)^{1/2} + d(J - 1/2)^{1/2} , \qquad (47b)$$

where a,b,c, and d are complex amplitudes for decay via partial waves $\ell = J-3/2$, $J-1/2$, $J+1/2$, and $J+3/2$ respectively. One may show that $\mathfrak{b}_2$ is of the form

$$\mathfrak{b}_2 = S \cos \lambda_0 - T \sin \lambda_0 \cos \Delta\phi , \qquad (48)$$

where $S, T, \Delta\phi$, and $\cos \lambda_0$ have the following values and where

$$|a|^2 + |c|^2 = 1, \quad |b|^2 + |d|^2 = 1, \quad \sin \lambda_0 \geqslant 0:$$

close up

#

J^P	S	T	$\Delta\phi$	$\cos \lambda_0$
$3/2^-, 5/2^+, 7/2^-$, etc.	$\lvert a\rvert^2 - \lvert c\rvert^2$	$2\lvert a\rvert\ \lvert c\rvert$	$\delta_c - \delta_a$	$(2J-3)/4J$
$3/2^+, 5/2^-, 7/2^+$, etc.	$\lvert b\rvert^2 - \lvert d\rvert^2$	$2\lvert b\rvert\ \lvert d\rvert$	$\delta_d - \delta_b$	$(-2J-5)/(4J+4$

We note that $-1 \leqslant b_2 \leqslant 1$, regardless of the magnitudes and relative phases of a,b,c, and d. If only the lower partial wave (a or b) contributes (for those cases having $J > 1/2$), b_2 has the following values:[43]

J^P	b_2	J^P	b_2
$1/2^+$	1.00	$1/2^-$	1.00
$3/2^-$	0.00	$3/2^+$	-0.80
$5/2^+$	0.20	$5/2^-$	-0.71
$7/2^-$	0.29	$7/2^+$	-0.67
limit $J \to \infty$	0.50	limit $J \to \infty$	-0.50

One expects the rate of decay via partial wave ℓ to be suppressed (relative to 1.0 for $\ell = 0$) by a factor of the order of[44]

$$(qR)^2 \, [1 + (qR)^2]^{-1} \qquad \text{for } \ell = 1 \qquad (49a)$$

$$(qR)^4 \, [9 + 3\,(qR)^2 + (qR)^4]^{-1} \qquad \text{for } \ell = 2 \qquad (49b)$$

$$(qR)^6 \, [225 + 45\,(qR)^2 + 6\,(qR)^4 + (qR)^6]^{-1} \qquad \text{for } \ell = 3, \qquad (49c)$$

where q is the momentum of $F_{3/2}$ in the F_J rest frame, and R is a characteristic radius of interaction, of the order of $(2m_\pi)^{-1}$. (For the decay process $\Xi^*(1817) \to \Xi^*(1530) + \pi$, $q = 230$ MeV/c $\approx 1/R$.) Taking $qR \approx 1$, we estimate $|D^2|/|S^2| \approx 0.08$ and $|F^2|/|P^2| \approx 0.007$, where S,P,D, and F are decay amplitudes for $\ell = 0,1,2$, and 3, respectively.

Even with complete ignorance of the relative phase $\Delta\phi$, we may specify the permitted range of the coefficient a_2, allowing for the presence of higher partial waves:

J^P	Partial waves ℓ	a_2
$1/2^+$	1	1.0
$1/2^-$	2	1.0
$3/2^-$	0,2	0.0 ± 0.5
$3/2^+$	1,3	-0.8 ± 0.1
$5/2^+$	1,3	0.2 ± 0.2

Decay via the higher partial wave is negligible for higher spin hypotheses.

V. ANALYSIS OF DATA

A. Decay parameters of the Ξ^-

Because the overall average polarization of our Ξ^- sample is small, the 2529 K-63 events were arbitrarily divided, according to final-state momentum, and values of $(\hat{\Xi}\cdot\hat{K})$, into 34 subsamples, defined in Table III-2. No attempt was made to optimize the binning criteria. Also listed, in 13 subsamples, are 902 events of the K-72 experiment, corresponding approximately to the sample analyzed earlier.[6,1] (The sample described in Ref. 1 contains additional events not in our K-72 sample, but polarization information from 3-body final states was not used.) In Table V-1 we compare results obtained separately from K-63 and K-72 data, and we present results from a combined sample containing 2529 + 902 = 3431 Ξ^- events.

Estimates of $\alpha_\Lambda\,\alpha_{\Xi^-}$ were obtained from maximum-likelihood fits to a decay distribution of the form Eq. (34); these estimates are independent of the assumed Ξ spin, and independent of the way in which subsamples are defined. Estimates of α_Λ, α_{Ξ^-}, and Φ_{Ξ^-} were obtained from fits to a decay distribution of the form (35); variable parameters in the fits were $\alpha_\Lambda, \alpha_{\Xi^-}$, Φ_{Ξ^-}, and the polarization of each subsample. Fits were performed (as indicated) both with α_Λ free, and with α_Λ weighted (by

Table V-1. Decay parameters for Ξ^-

α free

Sample	Events	$\alpha_\Lambda\alpha_\Xi$	Sub-samples	ℓnL	Fitted parameters α_Λ	α_Ξ	Φ_Ξ (deg)	Correlation matrix $(\alpha_\Lambda\alpha_\Xi)$	$(\alpha_\Lambda\Phi_\Xi)$	$(\alpha_\Xi\Phi_\Xi)$
K-63	2529	-0.262 ± 0.033	34	68.95	0.743 ± 0.122	-0.344 ± 0.063	10.1 ± 11.4	0.789	-0.027	-0.018
K-72	902	-0.281 ± 0.055	13	41.16	0.685 ± 0.107	-0.426 ± 0.067	9.7 ± 14.1	0.295	0.008	-0.020
Combined	3431	-0.267 ± 0.028	47	109.70	0.698 ± 0.069	-0.381 ± 0.045	10.0 ± 8.9	0.653	-0.026	-0.025
K-72[a]	1004[b]	--	12	38.74	0.682 ± 0.104	-0.362 ± 0.058	0.3 ± 10.6	0.295	0.027	0.015

$\alpha_\Lambda = 0.62\pm0.07$ included

Sample	Events	$\alpha_\Lambda\alpha_\Xi$	Sub-samples	ℓnL	Fitted parameters α_Λ	α_Ξ	Φ_Ξ (deg)	Correlation matrix $(\alpha_\Lambda\alpha_\Xi)$	$(\alpha_\Lambda\Phi_\Xi)$	$(\alpha_\Xi\Phi_\Xi)$
K-63	2529	-0.262 ± 0.033	34	68.53	0.656 ± 0.055	-0.375 ± 0.051	9.8 ± 11.6	0.404	-0.018	-0.015
K-72	902	-0.281 ± 0.055	13	41.02	0.641 ± 0.057	-0.432 ± 0.066	9.8 ± 14.3	0.099	0.010	-0.018
Combined	3431	-0.267 ± 0.028	47	109.41	0.657 ± 0.047	-0.394 ± 0.041	9.9 ± 9.0	0.383	-0.013	-0.019
K-72[a]	1004[b]	--	12	38.65	0.641 ± 0.056	-0.368 ± 0.057	0.5 ± 10.7	0.096	0.014	0.007

[a] Previously published results, included for comparison with our K-72 sample (see Ref. 1).
[b] includes 176 events providing information only on $\alpha_\Lambda\alpha_{\Xi^-}$.

a factor exp $[-1/2\ (\alpha_\Lambda - 0.62)^2/(0.07)^2]$ in the likelihood).[45]

Quoted errors on α_Λ, α_{Ξ^-}, and Φ_{Ξ^-} were obtained from the error matrix G, calculated as the negative of the inverse of the second-derivative matrix of $w = \ln \mathcal{L}$ (where the likelihood $\mathcal{L} = \prod_{i=1}^{N} I\,(\hat{\Lambda}_i, \hat{p}_i)$. If $x_1, x_2, \ldots$ are variable parameters in the maximum-likelihood fit, the error δx_i of a parameter x_i is given by

$$(\delta x_i)^2 = G_{ii} \qquad (50\,a)$$

$$\text{where } (G^{-1})_{jk} = \frac{\delta^2 w}{\delta x_i\ \delta x_j} \qquad (50\,b)$$

The correlation coefficients listed are off-diagonal elements of the normalized error matrix $C_{jk} = G_{jk}\,(G_{jj}G_{kk})^{-1/2}$. A study of Monte Carlo events[46] demonstrates that the calculated errors δx_i correspond to the rms deviation of independent measurements of x_i, i.e.

$$(\delta x_i)^2 = \langle (x_i - \langle x_i \rangle)^2 \rangle = \langle x_i^{\,2} \rangle - \langle x_i \rangle^2 \quad . \qquad (51)$$

In Fig. V-1 we illustrate the correlation between α_Λ and α_{Ξ^-}, for the combined K-72 and K-63 data. Correlations between α_Λ and Φ_{Ξ^-}, and between α_{Ξ^-} and Φ_{Ξ^-} are negligible.

As a visual check on the results presented we display certain angular correlations in the observed Ξ^- decay distributions.

In Fig. V-2 we display the distribution of $\hat{p}\cdot\hat{\Lambda}$ for the 3431 Ξ^- events listed in Table III-2. As expected, the observed distribution is proportional to $1 + \alpha_\Lambda \alpha_{\Xi^-} \hat{p}\cdot\hat{\Lambda}$ ~~$(\hat{p}\cdot\hat{\Lambda})$~~ with $\alpha_\Lambda \alpha_{\Xi^-} = -0.27$ (corresponding to the straight line plotted).

In Fig. V-3 we present distributions of the four quantities N (no. of events), $\sum_{i=1}^{N} (\hat{p}\cdot\hat{\Lambda})_i$, $\sum_{i=1}^{N} (\hat{p}\cdot\hat{y})_i$ and $\sum_{i=1}^{N} (\hat{p}\cdot\hat{x})_i$ as functions of $\hat{\Lambda}\cdot\hat{n} = \cos\theta$. For purposes of plotting, events in subsamples (see Table V-2) having $P_{\Xi} < 0$ (shaded) were rotated 180° about the beam axis, effectively raising the overall average polarization from 0.04 ± 0.04 to 0.26 ± 0.04 .

B. Spin of the Ξ

The existence, in the observed Ξ decay distribution, of any non-zero t_{LM} having $L > 1$ would immediately establish the Ξ spin J to be greater than 1/2. In Table V-2 we present, for 15 subsamples of Ξ^- and Ξ^0 events, values of t_{LM} obtained from maximum-likelihood fits assuming $J = 3/2$, $L_{max} = 3$, $\alpha_\Lambda = 0.62$, $\alpha_{\Xi^-} = \alpha_{\Xi^0} = -0.40$, $\Phi_{\Xi^-} = \Phi_{\Xi^0} = 0$. The Ξ^- data have been corrected for scanning biases, as explained in the Appendix (and in Appendix B of Reference 21). We compare values of $\ln\mathcal{L}$ from the $L_{max} = 3$ fits (seven parameters per sample) with values obtained assuming $L_{max} = 1$ (one parameter per sample). For the 15 samples, we observe an overall increase of 44.1 in $\ln\mathcal{L}$ as L_{max} is increased from 1 to 3. (An increase of

Table V-2. Search for J = 3/2 moments in Ξ decay.

	Subsample			N	$w = \ln \mathcal{L}$			t_{LM} (×100)						
	Expt.	Final state	p(BeV/c)		$L_{max}=1$	$L_{max}=3$	Δw	t_{10}	t_{20}	$\mathrm{Re}\, t_{22}$	$\mathrm{Im}\, t_{22}$	t_{30}	$\mathrm{Re}\, t_{32}$	$\mathrm{Im}\, t_{32}$
1.	K-72	Ξ^-K^+	1.2-1.4	194	4.8	5.9	1.1	-35±14	2±7	5±5	1±5	-7±8	-3±6	-4±6
2.	K-72	Ξ^-K^+	1.5	470	3.8	6.4	2.6	0±10	5±5	2±3	-2±3	-3±6	3±4	-6±4
3.	K-72	Ξ^-K^+	1.6, 1.7	166	6.5	8.5	2.0	40±17	-13±8	-2±5	0±5	7±9	2±7	-2±6
4.	K-63	Ξ^-K^+	1.7	272	7.4	11.0	3.6	27±12	-5±6	-7±4	-3±4	9±7	-4±5	-6±5
5.	K-63	Ξ^-K^+	2.1	342	4.9	8.7	3.8	17±11	-9±6	-4±4	-5±4	-7±6	-6±4	3±4
6.	K-63	Ξ^-K^+	2.45, 2.55	179	6.9	9.1	2.2	55±15	4±7	4±5	-5±5	4±8	-9±6	-2±6
7.	K-63	Ξ^-K^+	2.6, 2.7	229	7.7	10.1	2.4	47±14	4±7	3±5	2±5	12±8	8±5	-2±5
8.	K-72, K-63	$\Xi^-K^+\pi^0$	1.5-2.1	154	1.6	5.2	3.6	4±17	0±8	-1±6	-5±6	15±9	-3±6	12±7
9.	K-63	$\Xi^-K^+\pi^0$	2.45-2.7	301[a]	2.2	3.9	1.7	-18±13	-7±6	2±4	3±4	-7±7	0±5	0±5
10.	K-72, K-63	$\Xi^-K^0\pi^+$	1.5-2.1	367[a]	11.5	15.1	3.6	-31±11	4±5	0±4	-8±4	4±6	-3±4	2±4
11.	K-63	$\Xi^-K^0\pi^+$	2.45-2.7	473	8.0	14.3	6.3	-2±10	0±4	2±3	-6±3	-9±6	-6±4	7±4
12.	K-63	$\Xi^-K\pi\pi$	All	284	4.6	6.4	1.8	-27±13	3±6	1±5	-2±4	10±7	-3±5	-3±5
13.	K-72, K-63	Ξ^0K^0	All	194	1.2	4.7	3.5	-21±14	1±7	-3±5	13±5	0±8	-3±6	-1±6
14.	K-72, K-63	$\Xi^0K^+\pi^-$	1.5-2.1	164	2.8	4.2	1.4	0±16	7±8	3±6	-1±6	6±9	4±6	5±6
15.	K-63 K-63	$\Xi^0K^+\pi^-$ $\Xi^0K^0\pi^+\pi^-$	2.45-2.7 All	271 20	3.9	8.4	4.5	2±12	1±6	3±4	4±4	1±7	0±5	14±5
1-12		Ξ^- total		3431	69.9	104.6	34.7	2.6±3.6	-0.5±1.7	0.3±1.2	-3.0±1.2	0.6±2.0	-2.1±1.4	-0.1±1.4
13-15		Ξ^0 total		649	7.9	17.3	9.4	-5.3±8.1	2.5±3.9	1.0±2.7	5.6±2.7	1.9±4.7	0.3±3.2	7.2±3.2
1-15		Ξ^- and Ξ^0, total		4080	77.8	121.9	44.1	1.3±3.3	0.0±1.6	0.5±1.1	-1.6±1.1	0.8±1.8	-1.7±1.3	1.0±1.3

[a]Sample No. 9 contains eight K-72 $\Xi^-K^0\pi^+$.

45.0 is expected.) We conclude that the spin-1/2 hypothesis is permitted, although not required, by the data.

The spin-3/2 hypothesis could be discounted if one of the inequalities (13) or (15) were significantly violated. Although the spin-3/2 density matrix constraint (15) is violated by three subsamples (3, 6, and 7), the effect is less than one standard deviation in each case. Violation of the spin-5/2 density matrix constraint (16) is only slightly more significant.

Hence, only the presence of the (2J+1) factor in the transverse Λ polarization distribution (30c) affords us a possibility of spin discrimination.

(2J+1) Spin Factor

We have investigated the (2J+1) spin factor using 3278 K-72 and K-63 Ξ^- events. (Only 96% of the events appearing in Table III-1 were available at the time of this analysis.) The data were arbitrarily divided into 47 approximately equal subsamples according to final state, momentum, and c.m. Ξ production angle (see Table V-3. No attempt was made to optimize the binning criteria. Also listed in Table V-3 are seven Ξ^0 subsamples.

Maximum-likelihood fits were performed to an assumed Ξ decay distribution of the form (33) with (30); Λ variable parameters in the fits were α_Λ, α_{Ξ^-}, Φ_{Ξ^-}, and a value of t_{10}

Table V-3. Subsamples used in Ξ spin analysis (K-72 and K-63 data combined).

Subsample					
Final state	p(BeV/c)	Events	Sub-samples	Events per subsample	$(\hat{\Xi}\cdot\hat{K})$ cutoff points
Ξ^-K^+	1.2-1.4	194	3	65	0.69, 0.10
Ξ^-K^+	1.5	470	7	67	0.91, 0.78, 0.59, 0.29, -0.11, -0.51
Ξ^-K^+	1.6, 1.7	304	4	76	0.87, 0.65, -0.14
Ξ^-K^+	2.1	355	5	71	0.89, 0.76, 0.44, -0.44
Ξ^-K^+	2.45, 2.55	179	3	60	0.86, 0.26
Ξ^-K^+	2.6, 2.7	229	3	76	0.89, 0.50
$\Xi^-K^+\pi^0$	1.5-2.1	147	2	73	0.43
$\Xi^-K^+\pi^0$	2.45, 2.55	112	2	56	0.34
$\Xi^-K^+\pi^0$	2.6, 2.7	180	2	90	0.43
$\Xi^-K^0\pi^+$	1.5-2.1	350	5	70	0.69, 0.41, -0.02, -0.48
$\Xi^-K^0\pi^+$	2.45, 2.55	186	3	62	0.70, 0.07
$\Xi^-K^0\pi^+$	2.6, 2.7	288	4	72	0.78, 0.43, -0.17
$\Xi^-K^+\pi\pi$	all	135	2	68	0.29
$\Xi^-K^0\pi^+\pi^0$	all	149	2	74	-0.05
Ξ^- sample, total		3278	47	70	--
Ξ^0K^0	1.2-1.7 (K-72)	106	1	106	--
Ξ^0K^0	1.7-2.7 (K-63)	88	1	88	--
$\Xi^0K^+\pi^-$	1.5-1.7	70	1	70	--
$\Xi^0K^+\pi^-$	2.1	94	1	94	--
$\Xi^0K^+\pi^-$	2.45, 2.55	81	1	81	--
$\Xi^0K^+\pi^-$	2.6	112	1	112	--
$\Xi^0K^+\pi^-$ / $\Xi^0K^0\pi^+\pi^-$	2.7 / all	78 / 20	1	98	--
Ξ^0 sample, total		649	7	93	--

for each of the 47 subsamples. (The method of analysis is similar to the likelihood treatment of ~~References~~ Refs. 6 and 1.) Having found t_{20}, t_{22}, t_{30}, and t_{32} to be consistent with zero, we assumed $L_{max} = 1$ (i.e., $t_{20} = t_{22} = t_{30} = t_{32} = 0$); the assumption should not bias our determination of (2J+1). Fits were performed in three ways: (i) with no information regarding α_Λ or α_{Ξ^-}; (ii) with the use of $\alpha_\Lambda = 0.62 \pm 0.07$, the value of Cronin and Overseth;[45] (iii) with weighting of $\alpha_\Lambda = 0.62 \pm 0.07$ and $\alpha_\Lambda \alpha_{\Xi^-} = 0.321 \pm 0.048$, the latter value roughly corresponding to the world average of spin-independent determinations of $\alpha_\Lambda \alpha_{\Xi^-}$, excluding Berkeley data. ~~(These constraints were applied by~~ (Included in the likelihood $\mathcal{L}$ were factors of the form $\exp[-\frac{1}{2}(\alpha_\Lambda - 0.62)^2/(0.07)^2]$ and $\exp[-\frac{1}{2}(\alpha_\Lambda \alpha_{\Xi^-} + 0.321)^2/(0.048)^2]$.)

In Fig. V-4 we illustrate the behavior of $w = \ln\mathcal{L}$ as a function of the assumed spin factor (2J+1). From curve (ii) (α_Λ weighted by 0.62 ± 0.07, $\alpha_\Lambda \alpha_{\Xi^-}$ free) we estimate $(2J+1) = 2.0^{+0.7}_{-0.4}$, corresponding to a Ξ^- spin $J = 1/2$. (At the likelihood maximum, $\alpha_\Lambda = 0.65 \pm 0.05$, $\alpha_{\Xi^-} = -0.41 \pm 0.04$, and $\Phi_{\Xi^-} = 13^\circ \pm 9^\circ$.) The $J = 1/2$ hypothesis is favored over $J = 3/2$ by $\approx (2 \times 3.0)^{1/2} = 2.45$ times standard deviations; higher spin hypotheses are excluded by > 3 standard deviations. Violation of the spin-3/2 density matrix constraint in 16 subsamples causes a decrease of 7.03 in $w = \ln\mathcal{L}$ when the constraint is applied; however, the violation is not statistically

significant.[47]

Analysis of Monte Carlo Events

The conclusions above ~~of Sec. V.A. 2~~ were checked by comparing experimental data with samples of computer-generated Monte Carlo events. For comparison with the 15 Ξ^- and Ξ^0 subsamples of Table V-2, we generated 75 Monte Carlo samples, having 272 events each, according to each of the following hypotheses:

(a) $J = 1/2$, $\alpha_\Lambda = 0.62$, $\alpha_\Xi = -0.40$, $\Phi_\Xi = 0$, $t_{10} = 0$ (indistinguishable from $J = 3/2$ with $t_{10} = 0$);

(b) $J = 1/2$, $\alpha_\Lambda = 0.62$, $\alpha_\Xi = -0.40$, $\Phi_\Xi = 0$, $t_{10} = t_{10}^{max} = 0.57$;

(c) $J = 3/2$, $\alpha_\Lambda = 0.62$, $\alpha_\Xi = -0.40$, $\Phi_\Xi = 0$, $t_{10} = t_{10}^{max} = 0.43$.

For each sample, we performed two maximum-likelihood fits, assuming $\alpha_\Lambda = 0.62$, $\Phi_\Xi = 0$, and $J = 1/2$ and $3/2$, respectively; α_Ξ and t_{10} were free parameters in the fits. In Figs. V-5 and V-6 we present distributions of $X \equiv \Delta \ln \mathcal{L} \equiv \ln \mathcal{L}^{\#}(J = 1/2) - \ln \mathcal{L}^{\#}(J = 3/2)$ for the experimental data and for the Monte Carlo samples. See Ref. 21 for further discussion of Monte Carlo events and interpretation of likelihood results.

C. Analysis of $\Xi^*(1817) \to \Xi^*(1530) + \pi$

In this section we investigate the spin and parity of $\Xi^*(1817)$, using a cleaner sample of $\Xi^0 K^0 \pi^+ \pi^-$ events than that studied previously, and utilizing two spin

tests proposed by Button-Shafer.[30] (One of these has been previously applied.[9]) The scarcity of data prevents the use of more elaborate tests.

In Fig. V-7 we present a plot of $\Xi\pi$ mass squared vs. $\Xi\pi\pi$ mass squared for 164 $\Xi K\pi\pi$ events from the K-63 experiment. Six events are at 2.1 BeV/c, and the remainder are from 2.45 to 2.7 BeV/c. Plotted are 135 unambiguous events (78 $\Xi^- K^+\pi^+\pi^-$, 20 $\Xi^0 K^0\pi^+\pi^-$, and 37 $\Xi^- K^0\pi^+\pi^0$) with visible lambda decay, plus 29 $\Xi^- K^0\pi^+\pi^0$ events without visible lambda decay. Only the 135 unambiguous events are further analyzed. Events designated $\Xi^*(1817)$ have $\Xi\pi\pi$ effective masses between 1775 and 1850 MeV, corresponding to an interval of $\approx 2 \times \Gamma_{obs}$. Events designated $\Xi^*(1530)$ have at least one $\Xi\pi$ pair with $I_z = \pm 1/2$ and [1510 MeV $\leqslant m(\Xi\pi) \leqslant$ 1550 MeV]; events designated K^* have at least one $K\pi$ pair with $I_z = \pm 1/2$ and [840 MeV $\leqslant m(K\pi) \leqslant$ 940 MeV]. Of the events designated as both $\Xi^*(1817)$ and $\Xi^*(1530)$, about <u>half</u> are due to non-resonant background.

Using the extended Byers-Fenster formalism for hyperon decay into a spin-3/2 fermion plus a spin-zero boson (see Sec. IV and Ref. 30), and assuming the $\Xi^*(1530)$ to have spin 3/2, we examine the spin and parity [relative to $\Xi^*(1530)$] of $\Xi^*(1817)$ decaying via $\Xi^*(1817) \rightarrow \Xi^*(1530) + \pi$. The sample analyzed contains 41 unambiguous $\Xi K\pi\pi$ events (23 $\Xi^- K^+\pi^+\pi^-$, 13 $\Xi^- K^0\pi^+\pi^0$, and 5 $\Xi^0 K^0\pi^+\pi^-$) having both a $\Xi^*(1817)$ and a $\Xi^*(1530)$. Of the 13

$\Xi^- K^0 \pi^+ \pi^0$ events, 6 contain a $\Xi^{*0}(1530)$ and 7 contain a $\Xi^{*-}(1530)$; none contains both.

Let us designate as π_2 and π_1 the pions included and not included, respectively, in the $\Xi^*(1530)$; i.e.,

$$\begin{aligned} K^- + p &\to \Xi^*(1817) + K \\ &\quad\ \hookrightarrow \Xi^*(1530) + \pi_1 \\ &\qquad\qquad \hookrightarrow \Xi + \pi_2 \ . \end{aligned} \tag{52}$$

In the $\Xi^- K^0 \pi^+ \pi^0$ final state, either $K\pi_1$ or $K\pi_2$ may form a K^*, whereas in the $\Xi^- K^+ \pi^+ \pi^+$ and $\Xi^0 K^0 \pi^+ \pi^-$ final states, only $K\pi_1$ may form a K^*.

From the 41-event sample, in order to avoid interference effects between $\Xi^*(1817)$ and $K^*(890)$, we removed 21 events having $m(K\pi_1) > 840$ MeV. The 20 events remaining include 15 $\Xi^- K^+ \pi^+ \pi^-$, 4 $\Xi^- K^0 \pi^+ \pi^0$, and 1 $\Xi^0 K^0 \pi^+ \pi^-$. None of the 4 $\Xi^- K^0 \pi^+ \pi^0$ events remaining has a $K\pi_2$ effective mass in the K^* region.

In order that the angular distributions of interest be undistorted by the removal of K^* events, we assigned double weight to certain non-K^* events, selected as follows. For an event of the above type (Eq. (52), the K^* cutoff criterion $m(K\pi_1) > 840$ MeV may be re-expressed as a cutoff in $\cos\alpha \equiv \hat{\Xi}^*(1530) \cdot \hat{\Xi}^*(1817)$, where the cutoff point in $\cos\alpha$ depends upon the c. m. energy of the $K^- p$ system and upon the effective masses $m(\Xi\pi_1\pi_2)$ and $m(\Xi\pi_2)$ for the particular event. The curves plotted

in the left half of Fig. V-8 represent the relation between c.m. energy and the value of cos α corresponding to $m(K\pi_1) = 840$ MeV for events having both a $\Xi^*(1817)$ and a $\Xi^*(1530)$. In the right half of Fig. V-8 the same curves appear, reflected about the line cos α = 0. For each event we imagine a single curve (and its reflection) corresponding to the particular values of $m(\Xi\pi_1\pi_2)$ and $m(\Xi\pi_2)$ for that event. Each K^* event falls to the left of the left-hand curve and is discarded; in order to correct for the events lost, each event falling to the right of the reflected curve (on the right-hand side) is assigned double weight in the analysis to follow. In effect, some events having cos α < 0 are replaced by other events having cos α > 0. The removal-and-replacement procedure does not systematically bias either of the two experimental distributions of interest in the following analysis.

In Fig. V-9(a) we plot the distribution of $|\cos\theta| \equiv |\hat{\Xi}^*(1530) \cdot \hat{n}|$, where $\hat{n} = \hat{K}X\hat{\Xi}^*(1817)$ is the $\Xi^*(1817)$ production normal. Assuming $I(\theta)$ to be of the form $1 + a_2P_2(\cos\theta)$, we calculate the coefficient a_2 as

$$a_2 = 5\langle P_2\rangle = \left(\frac{5}{N'}\right)\sum_{i=1}^{N'} P_2(\cos\theta_i) \qquad (53)$$

with an experimental error

$$\delta a_2 = \left(\frac{5}{N}\right)^{1/2}\left[1 + \frac{2}{7}a_2 - \frac{1}{5}a_2^{\,2}\right]^{1/2}. \qquad (54)$$

(The a_2 is proportional to t_{20}, a measure of $\Xi^*(1817)$ alignment along $\hat{n}$.)

Here N (= 20) is the actual number of events, and N' (= 28) is the number with doubly weighted events counted twice. For the non-K^* events of Fig. V-9 we obtain $a_2 = 0.6 \pm 0.5$, consistent with isotropy and with the J = 1/2 assignment. However, we cannot rule out higher spin hypotheses. For $3/2^-$ ($3/2^+$) a_2 may have any value between -1.0 and 1.0 (-0.8 and 0.8). Background events lying outside the $\Xi^*(1817)$ region (1775 to 1850 MeV), but otherwise selected just as the $\Xi^*(1817)$ events, also yield an $I(\theta)$ distribution consistent with isotropy.

In Fig. V-9 (b) we plot the distribution of $|\cos\psi| \equiv |\hat{\Xi}\cdot\hat{\Xi}^*(1530)|$, i.e., the decay angle of $\Xi^*(1530)$ relative to its line of flight. The expected distribution is of the form $I(\psi) \propto 1 + b_2 P_2(\cos\psi)$ for any value of the $\Xi^*(1817)$ spin J. For a pure sample of $\Xi^*(1817)$ decaying via $\Xi^*(1817) \to \Xi^*(1530) + \pi$, predicted values of the coefficient b_2 are as follows [where the parity of the $\Xi^*(1817)$ is defined relative to that of the $\Xi^*(1530)$]:

J^P	Partial wave ℓ	b_2 predicted
$1/2^+$	1	1.0
$1/2^-$	2	
$3/2^-$	0,2	
$5/2^+$	1,3	≈ -0.5 to $+0.5$
$7/2^-$	2,4	
etc.	etc.	
$3/2^+$	1,3	
$5/2^-$	2,4	≈ -0.9 to -0.5
$7/2^+$	3,5	
etc.	etc.	

The observed value of b_2 is 1.4 ± 0.5, which favors the hypotheses $J^P = 1/2^{\pm}$ and $J^P = 3/2^-$, $5/2^+$, $7/2^-$, etc. over $J^P = 3/2^+$, $5/2^-$, $7/2^+$, etc. Simply from angular-momentum barrier-penetration arguments, the lower ℓ-wave hypotheses are more likely, so that the evidence points to $J^P = 3/2^-$ (with $\ell = 0$) as the most probable hypothesis.

Background events outside the Ξ^* (1817) region yield a value $b_2 = 0.2 \pm 0.4$, indicating that the observed anisotropy may indeed be associated with Ξ^*(1817). However, because the Ξ^* (1817) sample contains $\gtrsim$ 50% background, we cannot ignore the possibility that the anisotropy may be due to Ξ^* (1817) interference with nonresonant background. In conclusion, our analysis does not permit us to rule out conclusively any J^P hypothesis for Ξ^* (1817).

D. Results for Ξ^* (1530)

Events containing the Ξ^* (1530), of the type $\Xi K\pi$ and $\Xi K\pi\pi$, were also analyzed by likelihood techniques to determine the Ξ^*(1530) spin and parity. For the 251 Ξ^* from $\Xi K\pi$ final states (not previously reported), the $J = 1/2$ hypothesis is roughly 3 or 4% as likely as the $J = 3/2$ hypothesis. The hypothesis $J^P = 3/2^-$ is favored over $3/2^-$ by ≈ 2.1 standard deviations. For the Ξ^* (1530) events from $\Xi K\pi$ and $\Xi K\pi\pi$ samples combined, the spin result becomes 3.5% ($J = 1/2$ compared with 3/2) and $J^P = 3/2^-$ is favored over $3/2^-$ by ≈ 2.8 standard deviations. Thus little improvement over the results from the $\Xi K\pi\pi$ sample (Ref. 11) is obtained; spin discrimination is poorer than that of London et al. (1% for $J = 1/2$), but parity discrimination is better than that of Schlein et al. (0.035 confidence level for $3/2^-$).[3,2]

VI. DISCUSSION

A. Decay parameters of the Ξ^-

The values of Ξ^- decay parameters reported in Table V-1 are in agreement with previously published results obtained from K-72 data and from K-63 $\Xi^- K^+$ data.[1,6-8] The slight differences that exist are due to differences in the samples analyzed, in the binning criteria, and in the values assumed for α_Λ .

In Table VI-1 and Fig. VI-1 we compare values listed in Table V-1 with values previously reported in other experiments[1-5]; and we list approximate world averages of α_{Ξ^-} and Φ_{Ξ^-} . Because different assumed values of α_Λ were used in various experiments, and because α_Λ and α_{Ξ^-} are highly correlated, values of α_{Ξ^-} were not averaged directly. For non-Berkeley data, we calculated $\alpha_\Lambda \alpha_{\Xi^-} = -0.325 \pm 0.047$; then assuming $\alpha_\Lambda = 0.657 \pm 0.047$ we obtained $\alpha_{\Xi^-} = -0.495 \pm 0.080$ which was averaged with the Berkeley value $\alpha_{\Xi^-} = -0.394 \pm 0.041$ to obtain the world average listed.

The positive value of $\gamma_{\Xi^-} = (1 - \alpha_{\Xi^-}^2)^{1/2} \cos \Phi_{\Xi^-}$ shows that the S-wave (parity-violating) amplitude dominates in Ξ^- decay. The phase difference of S and P amplitudes, calculated from the Berkeley values of α_{Ξ^-} and Φ_{Ξ^-}, is $(\Delta_p - \Delta_s) = \tan^{-1} (\beta_{\Xi^-}/\alpha_{\Xi^-}) = 157^{\circ}{}^{+21^{\circ}}_{-25^{\circ}}$.[48] In the absence of final-state interactions, T invariance in the decay

Table VI-1. Decay parameters: comparison of experimental results.

Lab	Events Ξ^-	$\alpha_\Lambda\alpha_{\Xi^-}$	Fitted or assumed value of α_Λ	α_{Ξ^-}	Φ_{Ξ^-} (deg)
LRL(K-72)[a]	1004	--	0.641±0.056	-0.368 ±0.057	0.5±10.7
LRL(K-63)[b]	2529	-0.262 ±0.033	0.656 ±0.055	-0.375 ±0.051	9.8±11.6
LRL combined[b]	3431	-0.267 ±0.028	0.657 ±0.047	-0.394 ±0.041	9.9±9.0
BNL+S[c]	700	-0.34 ±0.09	0.62 ±0.07	-0.47 ±0.12	0±20
EP+[d]	517	-0.27 ±0.07	0.62 ±0.07	-0.44 ±0.11	-16±37
UCLA[e]	356	-0.41 ±0.10	0.62 ±0.07	-0.62 ±0.12	54±25
CERN[f]	62	-0.35 ±0.18	0.61	-0.73 ±0.21	45±30
Average[g]	5066	-0.28 ±0.02	0.66 ±0.05	-0.42 ±0.04	113±7.4

[a]See Ref. 1

[b]See Table V-VIII (bottom) of Ref. 21.

[c](Brookhaven National Laboratory and Syracuse University). See Ref. 3

[d](Ecole Polytechnique and others). See Ref. 4

[e]See Ref. 2

[f]See Ref. 5

[g]Only entries below dashed line are included in average. See text regarding values of α_{Ξ^-} .

transition requires $(\Delta_p - \Delta_s) = 0$ or π, whereas C invariance requires $(\Delta_p - \Delta_s) = \pm \pi/2$ [49]. It appears that the hypothesis of T invariance is favored by the data.

Under the assumptions of SU(3) symmetry, octet dominance, and invariance under R (i.e., inversion through the origin $I_z = 0$, $Y = 0$) Lee[50] has predicted a triangular relationship among the non-leptonic covariant decay amplitudes for the processes

$$\begin{aligned} \Xi_-^- &: \quad \Xi^- \to \Lambda + \pi^- \\ \Lambda_-^o &: \quad \Lambda^o \to p + \pi^- \\ \text{and} \quad \Sigma_0^+ &: \quad \Sigma^+ \to p + \pi^o \quad . \end{aligned} \tag{55}$$

According to Lee, both the S-wave (parity-nonconserving) and P-wave (parity-conserving) amplitudes satisfy the relationship

$$2\, \Xi_-^- - \Lambda_-^o = \sqrt{3}\, \Sigma_0^+ \quad . \tag{56}$$

The same relationship (for either parity-nonconserving or parity-~~non~~conserving amplitudes, or both) has been derived by other authors under different assumptions.[51]

Furthermore, the $|\Delta I| = 1/2$ rule predicts a triangle relation

$$\Sigma_0^+ = \frac{1}{\sqrt{2}} [\Sigma_-^- - \Sigma_+^+] \tag{57}$$

among amplitudes for the processes

$$\Sigma_0^+ : \quad \Sigma^+ \to p + \pi^0$$
$$\Sigma_+^+ : \quad \Sigma^+ \to n + \pi^+ \qquad (58)$$
$$\Sigma_-^- : \quad \Sigma^- \to n + \pi^- \quad ,$$

so that the Lee triangle prediction and the $|\Delta I| = 1/2$ rule together require

$$\frac{1}{\sqrt{3}} [2\, \Xi_-^- - \Lambda_-^0] = \frac{1}{\sqrt{2}} [\Sigma_-^- - \Sigma_+^+] \quad . \qquad (59)$$

In Eqs. (56), (57), and (59), the covariant S- and P-wave amplitudes (denoted by A and B, respectively) are related to the partial decay rate w by

$$w = \frac{q}{8\pi\, M^2} \left\{ |A|^2 \, [(M+m)^2 - \mu^2] + |B|^2 \, [(M-m)^2 - \mu^2] \right\} , \qquad (60)$$

where M, m, and μ are the rest masses of the parent baryon, the decay baryon, and the decay pion, respectively, and q is the pion momentum in the rest frame of the parent baryon. In terms of the phenomenological decay amplitudes a and b appearing in Eq. (28), A and B are given by

$$\left(\frac{B}{A}\right)^2 = \left(\frac{b}{a}\right)^2 \left[\frac{(M+m)^2 - \mu^2}{(M-m)^2 - \mu^2} \right] \quad . \qquad (61)$$

A recent determination of the Σ decay parameters $\alpha(\Sigma_0^+)$, $\alpha(\Sigma_+^+)$, and $\alpha(\Sigma_-^-)$ has demonstrated that (57) is well satisfied,[52] and also permits a more ~~accurate~~ exacting test of Eqs. (56) and (59) than was previously possible.[1,53] In Table VI-2 we present covariant amplitudes A and B for the processes of (55) and (58), calculated under the assumption that A and B are

Table VI-2. Non-leptonic hyperon decay amplitudes

(Center for A and B)

Decay	τ $\times 10^{10}$ sec^{-1}	Branching fraction	α	A^a $\times 10^{-5}$ (sec·m_π)$^{1/2}$	B^a	(A,B) Correlation coefficient
$\Xi^-_-(\Xi^- \to \Lambda + \pi^-)$	1.75±0.05	1.00	-0.394±0.041	2.022±0.029	-6.70±0.66	0.136
$\Lambda^o_-(\Lambda \to p + \pi^-)$	2.53±0.05	0.663±0.014	0.657±0.047	1.542±0.030	10.85±0.97	-0.532
$\Sigma^+_o(\Sigma^+ \to p + \pi^o)$						
$\gamma > 0$	0.810±0.013	0.528±0.015	-0.960±0.067	1.558±0.142	-11.71±1.88	-0.959
$\gamma < 0$				1.168∓0.187	-15.61∓1.42	
$\Sigma^+_+(\Sigma^+ \to n + \pi^+)$						
$\gamma > 0^a$	0.810±0.013	0.472±0.015	-0.006±0.043	-1.861±0.034	- 0.05±0.41	-0.001
$\gamma < 0$				-0.005∓0.040	19.08∓0.35	
$\Sigma^-_-(\Sigma^- \to n + \pi^-)$						
$\gamma > 0$	1.654±0.031	1.00	-0.017±0.042	1.863±0.017	-0.15±0.39	-0.016
$\gamma < 0$				0.015∓0.039	-18.34∓0.17	
$\frac{1}{\sqrt{3}}(2\,\Xi^-_- - \Lambda^o_-)$	--	--	--	1.455±0.040	-14.09±0.70	0.004
$\frac{1}{\sqrt{2}}(\Sigma^-_- - \Sigma^+_+)$						
$\gamma(\Sigma^-_-) > 0,\ \gamma(\Sigma^+_+) < 0$	--	--	--	1.321±0.031	-13.60±0.37	0.005
$\gamma(\Sigma^-_-) < 0,\ \gamma(\Sigma^+_+) > 0^b$				1.327±0.037	-13.01±0.31	0.005

The m_π can be disregarded if the q of Eq. 60 is expressed in units of $m_\pi c$.

This solution is inconsistent with recent evidence that $\gamma(\Sigma^+_+) < 0$. See Ref. 55.

relatively real.[54] Only the relative signs of A and B are experimentally observable; a further ambiguity exists in the case of the Σ^+_0 and Σ^-_- decays [(55) and (58)], where the sign of γ has not been determined. A recent experiment has shown that $\gamma < 0$ for Σ^+_+ decay.[55] In Table VI-2, world-average values of lifetimes, branching fractions, and decay parameters are used,[56] except that α_{Ξ^-} and α_Λ are our results from K-63 and K-72 data.

The consistency of the data with Eqs. (56), (57), and (59) is illustrated in Fig. VI-2. In plotting the error ellipse for $(2\,\Xi^-_- - \Lambda^0_-)/\sqrt{3}$, we have taken into account the correlation between α_{Ξ^-} and α_Λ. We conclude that Eqs. (56) and (57) are well satisfied by the experimental data; Eq. (59) is less well satisfied. [Fig. VI-2 actually represents Ξ^-_- and Λ^0_- amplitudes derived from $\alpha_{\Xi^-} = -0.381 \pm 0.037$ and $\alpha_\Lambda = 0.690 \pm 0.048$. Our A_Ξ and A_Λ (Table VI-2) differ from these by $< 1\%$, whereas B_Ξ is larger (3.7%) and B_Λ smaller (5.5%); thus our Table VI-2 values yield a slightly better fit to the triangle hypothesis, in that point 1 is moved up by $\approx 1\%$ of its B coordinate.]

A veritable flood of predictions concerning non-leptonic hyperon decay has resulted from the advent of SU(6) and higher symmetry schemes. (As of August, 1966, at least 70 papers containing specific predictions regarding decay amplitudes have appeared in the literature. Most of these deal with the Lee SU(3) triangle prediction and the reasons for its apparent validity.) The theoretical situation is far too complex to discuss here, and the reader is referred to a recent review by Pais.[57] Predictions of various theoretical models may be readily

B. Spin of the Ξ

Our conclusion that the Ξ has spin 1/2 is in agreement with the prediction of SU(3) and with the findings of previous investigations. A maximum-likelihood analysis identical with that of Sec. V. B. performed on 828 K-72 $\Xi^- K^+$ events alone, yields a value $X = \ln\mathcal{L}(1/2) - \ln\mathcal{L}(3/2) = 2.60$, favoring the spin-1/2 hypothesis by 2.3 standard deviations.[1] (Our analysis of 3278 events yields only slightly better spin discrimination (2.45 s.d.), partly because K-63 events are not strongly polarized and partly because we have not optimized the binning criteria, as was done in Ref. 1. See Fig. VI-3.

In an alternative approach, one may calculate directly the factor (2J+1) as a ratio of odd-L moments of the transverse and longitudinal Λ polarization distributions.[28, 29, 2, 30, 1] If only moments proportional to t_{10} are considered,

$$2J+1 = \frac{\left[\langle \underset{\sim}{P}\cdot\hat{y}\sin\theta\rangle^2 + \langle \underset{\sim}{P}\cdot\hat{x}\sin\theta\rangle^2\right]^{\frac{1}{2}}}{(1-\alpha_\Xi^2)^{\frac{1}{2}}\,\langle \underset{\sim}{P}\cdot\hat{\Lambda}\cos\theta\rangle} \qquad (62)$$

For 356 Ξ^- events, Carmony et al.[2] obtained a value (2J+1) = 1.53, assuming $\alpha_{\Xi^-} = -0.48$. By calculating an expected distribution in (2J+1) (presumably assuming the numerator and denominator of Eq. (62) to be normally distributed quantities) they claim an exclusion of the spin-3/2 hypothesis by 3.1 standard deviations.

For 749 Ξ^- events of the K-72 experiment, Button-Shafer et al. obtained values of (2J+1) = 2.86 and 2.18, assuming

$\alpha_{\Xi^-} = -0.48$ and -0.34, respectively.[6,1] Here the 2J+1 values and their expected distributions were calculated as the ratio of two normally distributed quantities.[58] The resulting confidence levels, with α_{Ξ^-} assumed to be -0.48 (-0.34), were 0.22 (0.42) for J = 1/2, 0.15 (0.015) for J = 3/2, and 0.003 (0.0002) for J = 5/2.

C. $\Xi^*(1817)$ classification.

Our results from the analysis of $\Xi^*(1817) \rightarrow \Xi^*(1530) + \pi$ are consistent with those obtained in previous investigations. The hypotheses $J^P = 1/2^{\pm}$, $3/2^-$, $5/2^+$, $7/2^-$, etc. are favored over others, but any assignment from our data is questionable because of large background. ($J^P = 3/2^-$ might be considered the most likely. See discussion near the end of Sec. V.C.)

In an earlier analysis[9] of essentially the same data, the distribution appearing in Fig. V-9(a) was found to be consistent with isotropy. In the same analysis, the observed branching ratios of $\Xi^*(1817)$ into

$\Xi^*(1530) + \pi$, $\Lambda + \bar{K}$, and $\Xi + \pi$ were cited as evidence possibly favoring the $J^P = 3/2^-$ and $5/2^+$ hypotheses. (More recent information regarding branching ratios renders the same test somewhat less conclusive than it was considered earlier.)

In Ref. 10 Button-Shafer et al. performed a Byers-Fenster moment analysis of $\Xi^*(1817)$ (in K-63 $\Lambda K\bar{K}$ final states) decaying into $\Lambda + \bar{K}$. [We disregard a similar analysis of $\Xi^*(1817) \to \Xi + \pi$, as it is now believed that the $\Xi\pi$ enhancement near 1817 MeV may be entirely due to $\Xi^*(1933)$.] [22] The analysis of $\Xi^*(1817)$ in $\Lambda K\bar{K}$ final states is complicated by the presence of interfering ϕ (1020) and (in $\Lambda K^o\overline{K^o}$ final states) by the impossibility of distinguishing K^o from $\overline{K^o}$. After removal of events in the ϕ (1020) region, 71 (resonant plus background) events in the region [1775 MeV $\leqslant m(\Lambda\bar{K}) \leqslant$ 1850 MeV] were found to require 'spin' > 1/2, with the hypothesis $J^P = 3/2^-$ slightly preferred over $3/2^+$. However, no firm conclusions could be drawn; i.e. "background events outside the $\Xi^*(1820)$ region also require a 'spin' greater than 1/2, but perhaps not so firmly as do the 'resonant' events," and "the evidence (for $J^P = 3/2^-$ over $3/2^+$) is exceedingly weak because of large background in the $\Xi^*(1820)$ decay channels." [10]

We have attempted a maximum-likelihood analysis of a somewhat larger $\Lambda K\bar{K}$ data sample than that analyzed

earlier. Here we removed events containing ϕ (1020) by requiring $(\hat{\Lambda} \cdot \hat{\Xi}^*(1817)) \leq 0$, whereas in the previous analysis (due to statistical limitations) only events in a narrow ϕ band were removed . For 59 events in the region [1787 MeV $\leq m(\Lambda\bar{K}) \leq$ 1847 MeV] we obtain values of $w = \ln\chi = 0.00$, 1.01, 3.36, and 3.66 for $J^P = 1/2^-$, $1/2^+$, $3/2^+$, and $3/2^-$, respectively. An increase of 3.0 is to be expected as J is increased from 1/2 to 3/2, simply from the addition of six extra parameters, so that our analysis of $\Xi^*(1817) \to \Lambda + \bar{K}$ provides no spin or parity discrimination whatever. [Comparable results are obtained for background events outside the $\Xi^*(1817)$ region.]

No evidence has been found for a Ξ^* resonance near 1600 MeV, which had been suggested as the missing member of a $3/2^-$ unitary octet containing the $N^*_{1/2}$ (1525), the Y^*_0 (1520), and the Y^*_1 (1660). (The last is not firmly established as a $3/2^-$ state.)

Dalitz has suggested perhaps the most attractive scheme to accommodate the $\Xi^*(1817)$, if it has spin and parity $3/2^-$.[59] The $N^*_{1/2}$ (1525), Y^*_0 (1520), Y^*_1 (1660), and $\Xi^*_{1/2}$ (1817) could form an octet, with the singlet Y^*_0 mixing with a new $3/2^-$ singlet state at perhaps 1670 MeV. However, as indicated above, other classifications are certainly possible for the $\Xi^*(1817)$ [and perhaps for the $Y^*(1660)$].

VII. ACKNOWLEDGMENTS

Dr. Peter Berge has furnished useful programming assistance and much helpful advice. Thanks are due to Dr. Joseph Murray, who supervised the beam design and construction. The Bevatron and bubble-chamber crews, and also Alvarez Group Scanners and Measurers have provided indispensable services. We have appreciated the interest of Dr. Arthur Rosenfeld. Finally we thank Dr. Luis Alvarez for his encouragement.

APPENDIX: DISCUSSION OF SYSTEMATIC ERRORS

In Fig. A-1 we present, for the 3431 Ξ^- events of Table III-2, distributions of $\hat{\Lambda}\cdot\hat{K}$ and $\hat{\Lambda}\cdot\hat{\Xi}$. These distributions should be isotropic if $J_{\Xi} = 1/2$ and if scanning biases and other systematic effects are absent. (Even if $J_{\Xi} > 1/2$, these distributions must be even in $\hat{\Lambda}\cdot\hat{K}$ and $\hat{\Lambda}\cdot\hat{\Xi}$.)

We attempt to determine the exact cause of the observed anisotropy, in order to see whether it can bias our measurement of Ξ^- decay parameters. The following effects are considered:

(i) loss of events having π^- (from Ξ^- decay) nearly collinear with Ξ^- ;

(ii) loss of events having short Ξ^- and/or Λ ;

(iii) escape from chamber, prior to decay, of Ξ^- or Λ ;

(iv) precession of Ξ^- and/or Λ polarization in magnetic field.

In order to facilitate our discussion we define two new coordinate systems, $(\hat{x},\hat{y},\hat{z})$ and $(\hat{x}',\hat{y}',\hat{z}')$. The axes $\hat{z}$ and $\hat{z}'$ correspond to $\hat{p}_k(\text{lab})$ and $\hat{p}_{\Xi}(\text{lab})$ respectively, the lab directions of the incident K^- and of the Ξ^-. We define $\vec{y} = \hat{p}_k(\text{lab}) \times \hat{z}_{ch}$ and $\vec{y}' = \hat{p}_{\Xi}(\text{lab}) \times \hat{z}_{ch}$, where $\hat{z}_{ch}$ is the bubble chamber z-axis (essentially the optic axis and the direction of the magnetic field).[60] Directions of particles with respect to (x,y,z) and

(x',y',z') are specified by angles (θ,ϕ) and (θ',ϕ') respectively. Incident beam tracks are nearly horizontal in the bubble chamber (i.e., $\hat{x} \approx \hat{z}_{ch}$), so we may regard $\psi^{(lab)}$ and $\psi'^{(lab)}$ (projected angles in the y-z plane) as the projected angles (relative to $\hat{p}_k^{(lab)}$ and $\hat{p}_\Xi^{(lab)}$, respectively) seen by the scanner.

1. Small-angle Ξ^- decay. In Figs. A-2 and A-3 we present, for the 2529 K-63 Ξ^- events listed in Table III-1, scatter plots and projections of $\phi_\Xi^{(c.m.)}$ vs. $\cos\theta_\Xi^{(c.m.)}$, angles describing Ξ production in the c.m. frame, relative to axes (x,y,z); and $\phi_\Lambda'^{(\Xi)} = (\phi_\pi'^{(\Xi)} + \pi)$ vs. $\cos\theta_\Lambda'^{(\Xi)} = -\cos\theta_\pi'^{(\Xi)}$, angles describing Ξ decay in the Ξ rest frame, relative to axes (x',y',z'). The quantity $\cos\theta_\Xi^{(c.m.)}$ is equivalent to $(\hat{\Xi}\cdot\hat{K})$ as defined by Fig. IV-1; however, $\cos\theta_\Lambda'^{(\Xi)}$ is not exactly equivalent to $(\hat{\Lambda}\cdot\hat{\Xi})$, because for Fig. A-3 we have transformed $\vec{p}_\Lambda$ from the lab frame to the Ξ rest frame via a single Lorentz transformation along $\vec{p}_\Xi^{(lab)}$ (rather than through the intermediate c.m. frame).[61, 62] In Fig. A-3, $\phi_\Lambda'^{(\Xi)} \equiv \phi_\Lambda'$ (lab); i.e. $\phi_\Lambda' = \tan^{-1}(\hat{p}_\Lambda \cdot \hat{y}')/(\hat{p}_\Lambda \cdot \hat{x}')$ is the same in the Ξ rest frame as in the lab frame.

The distribution of $\phi_\Xi^{(c.m.)}$ in Fig. A-2 is consistent with isotropy. Hence, because the Ξ can be polarized only along $\vec{n} = (\hat{K} \times \hat{\Xi})$ and because $\hat{n}$ is uncorrelated with the bubble chamber z-axis, the distribution in Fig. A-3 should be isotropic if the Ξ has spin 1/2 and if systematic biases are absent. [Even if $J_\Xi > 1/2$, the distribution must be even in $\cos\theta_\Lambda'^{(\Xi)}$.]

We have sketched on the scatter plot (Fig. A-3), for $p_{\Xi}^{(lab)} = 1.0$ and 2.4 BeV/c, contours representing $\psi_{\pi}^{'(lab)} = 5^{o}$, where $\psi_{\pi}^{'(lab)}$ is the projected lab angle between the Ξ^{-} and decay pion at the Ξ^{-} decay vertex.[63] The curve in the $\cos\theta_{\Lambda}^{'(\Xi)}$ projection represents the expected distribution of events, calculated under the assumption that no events having $\psi_{\pi}^{'(lab)} \leq 5^{o}$ are detected. The observed distribution is consistent with assumed cutoff values $[\psi_{\pi}^{'(lab)}]_{min} = 5^{o} \pm 2^{o}$, corresponding to a 10 to 20% loss of events.

The observed anisotropy in $\hat{\Lambda}\cdot\hat{K}$ and $\hat{\Lambda}\cdot\hat{\Xi}$ (Fig. A-1) is related to the anisotropy in $\cos\theta_{\Lambda}^{'(\Xi)}$ (Fig. A-3), and may be entirely attributed to the loss of small-angle π^{-} from Ξ^{-} decay. As would be expected from such a bias, the anisotropy is most evident in $\cos\theta_{\Lambda}^{'(\Xi)}$, less so in $\hat{\Lambda}\cdot\hat{K}$, and still less so in $\hat{\Lambda}\cdot\hat{\Xi}$.[62]

Correcting for such a bias is somewhat difficult. For example, if one attempts to remove all events having $\psi_{\pi}^{'(lab)}$ less than some minimum value, say 5°, applying a weight to the remaining events, one inevitably loses <u>all</u> events in a finite range of $\cos\theta_{\Lambda}^{'(\Xi)}$ near $\cos\theta_{\Lambda}^{'(\Xi)}$.

As a substitute measure, we have corrected the anisotropy in $\hat{\Lambda}\cdot\hat{K}$ (Fig. A-1) by weighting events with an empirical correction factor of the form

$$w(z) = [1 - C(z - z_{0})^{2}]^{-1} \qquad (63)$$

where $z = (\hat{\Lambda}\cdot\hat{K})$, $z_{0} = -0.35$, and $C = 0.50$ (1.24) for

K-72 (K-63) events. (The curve plotted in Fig. A-1 corresponds to $[w(z)]^{-1}$.) After correction, the distributions in $\hat{\Lambda}\cdot\hat{K}$ and $\hat{\Lambda}\cdot\hat{\Xi}$ (Fig. A-1) are consistent with isotropy. The changes in measured decay parameters resulting from the correction are insignificant compared with statistical errors.[64]

The loss of small-angle Ξ decays obviously distorts the observed distribution of $\phi_\Lambda^{'(\Xi)}$ as well as $\cos\theta_\Lambda^{'(\Xi)}$, but because we average over $\phi_\Lambda^{'(\Xi)}$ the distortion does not bias our determination of Ξ^- decay parameters.

2. Short Ξ^- and/or Λ.

Because the forward-produced Ξ^- have greater lab momenta and thus travel farther prior to the decay, on the average, than do backward-produced Ξ^-, one expects a preferential loss of backward-produced Ξ^-, which distorts the observed Ξ^- production distribution (Fig. A-2). The loss rate is about 6% in K-72 events[1] and is most likely lower in K-63 events, where Ξ^- momenta are higher. However, loss of short Ξ^- cannot explain the anisotropy observed in the Ξ^- decay distribution (Figs. A-1 and A-3).

Due to the loss of short Λ, one also expects a preferential depletion of events having small values of $\cos\theta_\Lambda^{'(\Xi)}$.[62] Noting that $\vec{p}_\Lambda^{(lab)}/m_\Lambda \approx \vec{p}_\Xi^{(lab)}/m_\Xi$ (an approximation valid to about 10% in magnitude and 10° in angle for the events of this experiment) and that $\gamma_\Lambda^{(\Xi)} = E_\Lambda^{(\Xi)}/m_\Lambda \approx 1$, we may approximately write

$$p_\Lambda^{'(lab)} \approx \vec{p}_\Lambda^{(lab)} \cdot \hat{p}_{\Xi'}^{(lab)}$$

eta

$$\approx \eta_{\Xi'}^{(lab)} E_\Lambda^{(\Xi')} + \gamma_{\Xi'}^{(lab)} p_\Lambda^{(\Xi')} \cos\theta_\Lambda^{'(\Xi')} \qquad (64)$$

$$\approx M_\Lambda \eta_{\Xi'}^{(lab)} \left[1 + \frac{\beta_\Lambda^{(\Xi')}}{\beta_{\Xi'}^{(lab)}} \cos\theta_\Lambda^{'(\Xi')}\right]$$

$$\approx M_\Lambda \eta_\Lambda^{(lab)} \left[1 + \frac{\beta_\Lambda^{(\Xi')}}{\beta_{\Xi'}^{(lab)}} \cos\theta_\Lambda^{'(\Xi')}\right]$$

where $(\vec{\eta}_{\Xi'}^{(lab)}, \gamma_{\Xi'}^{(lab)}) = \frac{1}{m_{\Xi'}} (\vec{p}_{\Xi'}^{(lab)}, E_{\Xi'}^{(lab)})$ and $(\vec{\eta}_\Lambda^{(\Xi')}, \gamma_\Lambda^{(\Xi')}) = \frac{1}{m_\Lambda} (\vec{p}_\Lambda^{(\Xi')}, E_\Lambda^{(\Xi')})$

refer to the Ξ' in the lab frame and to the Λ in the Ξ' rest frame respectively. The Λ detection efficiency is approximately of the form (if Λ dip angle is ignored)

$$\exp\left[-\ell_{min}\, m_\Lambda / p_\Lambda^{(lab)}\, c\, \tau_\Lambda\right]$$

$$\approx 1 - \frac{\ell_{min}}{\eta_\Lambda^{(lab)}\, c\, \tau_\Lambda} \left[1 - \frac{\beta_\Lambda^{(\Xi')}}{\beta_{\Xi'}^{(lab)}} \cos\theta_\Lambda^{'(\Xi')}\right] \qquad (65)$$

where ℓ_{min} is an effective short-Λ cutoff length and T_Λ is the Λ lifetime. The overall loss rate ($\approx \ell_{min}/N_\Lambda^{(lab)}\, c\, \tau_\Lambda$) is of the order of 2% for K-72 events[1] and most likely smaller for K-63 events; the quantity $\beta_\Lambda^{(\Xi')}/\beta_{\Xi'}^{(lab)}$ is typically of the order of 0.15. Hence the expected asymmetry in $\cos\theta_\Lambda^{'(\Xi')}$ is of the order of 0.003 (to be compared with a statistical error of 0.011). We conclude that the anisotropy in $\cos\theta_\Lambda^{'(\Xi')}$ caused by the loss of short Λ is negligible in comparison with the anisotropy resuting from

other causes (e.g., small angle Ξ^- decay), and may be neglected in the analysis of Ξ^- decay. We have verified that application of a length cutoff for short Ξ^- and/or Λ (with appropriate weighting) does in fact produce a negligible change in measured values of Ξ^- decay parameters.

3. Escape Losses.

Due to the escape from the chamber prior to decay, one expects a preferential loss of forward-produced Ξ^- and of events having large values of $\cos\theta_\Lambda^{'(\Xi)}$. The loss of high-momentum Ξ^- can affect the Ξ^- production distribution (Fig. A-2) but not the Ξ^- decay distribution (Fig. A-3).

By a crude calculation taking into account the spatial distribution of the beam and the distribution of Λ lab momenta,[64] we estimate the asymmetry in $\cos\theta_\Lambda^{'(\Xi)}$ resulting from the loss of high-energy Λ to be of the order of 0.002 (to be compared with a statistical error of 0.011). The effect is comparable with that from the loss of short Λ and of opposite sign, and likewise may safely be neglected in the analysis of Ξ^- decay.

4. Precession of Ξ and Λ polarization.

As a function of time t, the precession of the polarization vector P(t) of a particle in a magnetic field $\vec{H}$ is described by

$$\dot{\vec{P}}(t) = \frac{d\vec{P}(t)}{dt} = \vec{\omega}(t) \times \vec{P}(t) . \qquad (66)$$

(Here $\vec{P}$ is the polarization three-vector defined in the particle's rest frame, and t is measured in the lab frame.) As discussed by Simmons,[65] the effective angular precession velocity $\vec{\omega}(t)$ may be considered as consisting of two terms:

$$\vec{\omega}(t) = \vec{\omega}_{\text{Larmor}} + \vec{\omega}_{\text{Thomas}}(t) \tag{67}$$

where

$$\vec{\omega}_{\text{Larmor}} = \frac{-\mu}{J} \frac{e_p}{2m_p c} \vec{H} \tag{68}$$

represents the Larmor precession of a particle at rest, and

$$\vec{\omega}_{\text{Thomas}}(t) = \frac{\gamma-1}{v^2} [\dot{\vec{v}}(t) \times \vec{v}(t)] , \tag{69}$$

called the Thomas precession, is a relativistic effect caused by the acceleration of the particle (if charged) in the magnetic field. Here

μ = magnetic moment in units of the Bohr nuclear magneton $e_p h/2m_p c$ (e_p and m_p are the proton charge and mass),

J = spin in units of h,

γ = (total lab energy/rest mass), and

$\vec{v}(t)$ = particle velocity in the lab frame, described by $\dot{\vec{v}}(t) = \frac{e}{\gamma mc} \vec{v}(t) \times \vec{H}$,

where e and m are the (signed) charge and mass of the particle in question. Hence

$$\vec{\omega}(t) = C_1 H + C_2 [\hat{H} \cdot \hat{v}(t)] \hat{v}(t) , \tag{70}$$

where[66]

$$C_1 = [\frac{-\mu}{2J} \frac{e_p}{m_p c} + \frac{\gamma-1}{\gamma} \frac{e}{mc}] H$$
$$C_2 = -(\frac{\gamma-1}{\gamma}) \frac{e}{mc} H . \tag{71}$$

Assuming for magnetic moments the mass-corrected SU(3) values[67]

$\mu_{\Xi^-} = -0.66$, $\mu_{\Xi^0} = -1.32$, and $\mu_\Lambda = -0.78$, one obtains

$$\text{for } \Xi^-: \quad C_1 = [0.66 - 0.71 \frac{\gamma-1}{\gamma}] \frac{e_p}{m_p c} H$$
$$C_2 = [0.71 \frac{\gamma-1}{\gamma}] \frac{e_p}{m_p c} H \tag{72}$$

$$\text{for } \Lambda: \quad C_1 = [0.78] \frac{e_p}{m_p c} H; \quad C_2 = 0 \tag{73}$$

$$\text{where } \frac{e_p}{m_p c} H = 9.58 \times 10^3 \text{ sec}^{-1} \text{ gauss}^{-1} \times 17.9 \text{ k gauss}$$
$$= 1.71 \times 10^8 \text{ sec}^{-1} . \tag{74}$$

Precession angles prior to decay are small (of the order of 10° or less), so to a good approximation we may ignore the variation of $\hat{v}(t)$ as a function of time; during a time interval $dt = \gamma d\tau$ (where τ is proper time), $\vec{P}(t)$ changes by approximately

$$d\vec{P} \approx C_1 \hat{H} \times \vec{P}(0) + C_2 [\hat{H} \cdot \hat{v}(0)] \hat{v}(0) \times \vec{P}(0) \; dt , \tag{75}$$

where $\hat{v}(t)$ and $\vec{P}(t)$ are evaluated at $t = 0$, the instant of Ξ production or decay, for Ξ and Λ, respectively.

(i) <u>Precession of Ξ^- polarization</u>.

At time $t = 0$, the Ξ have direction $\hat{v}(0) = \hat{\Xi}$, and

polarization $\vec{P}(0) = \vec{P}_\Xi = P_0\hat{n}$ along the production normal $\hat{n} = (\hat{K} \times \hat{\Xi})$. (As in Fig. IV-1, $\hat{K}, \hat{\Xi}$, and $\hat{n}$ are defined in the production c.m.; $\hat{H}$ is defined in the lab frame.) After an interval $dt = \gamma d\tau$, the Ξ will have acquired a longitudinal polarization component (relative to axes defined at production)[66] given by

$$d\vec{P}_\Xi \cdot \hat{\Xi} = P_0[C_1(\hat{H} \times \hat{n} \cdot \hat{\Xi}) + C_2(\hat{H} \cdot \hat{\Xi})(\hat{\Xi} \times \hat{n} \cdot \hat{\Xi})]\,\gamma d\tau$$

$$= P_0\, C_1(\hat{H} \times \hat{n} \cdot \hat{\Xi})\,\gamma d\tau \qquad (76)$$

$$= P_0\, C_1 \cos\theta_\Xi^{(c.m.)} \cos\phi_\Xi^{(c.m.)}\,\gamma d\tau\,,$$

and a component along $(\widehat{\Xi \times n}) = (\hat{\Xi} \times \hat{n})$ given by

$$d\vec{P}_\Xi \cdot (\widehat{\Xi \times n}) = P_0[C_1(\hat{H}\times\hat{n}) \cdot (\hat{\Xi}\times\hat{n}) + C_2(\hat{H}\cdot\hat{\Xi})(\hat{\Xi}\times\hat{n}) \cdot (\hat{\Xi}\times\hat{n})]\,\gamma d\tau$$

$$= P_0(C_1 + C_2)(\hat{H} \cdot \hat{\Xi})\,\gamma d\tau \qquad (77)$$

$$= P_0(C_1 + C_2) \sin\theta_\Xi^{(c.m.)} \cos\phi_\Xi^{(c.m.)}\,\gamma d\tau\,,$$

where $\theta_\Xi^{(c.m.)}$ and $\phi_\Xi^{(c.m.)}$ define the direction of the Ξ in the production c.m., as illustrated in Fig. A-1. As the production of events is uniform about the beam axis, the average precession angles

$$\left\langle \frac{d\vec{P}_\Xi \cdot \hat{\Xi}}{P_0} \right\rangle \quad \text{and} \quad \left\langle \frac{d\vec{P}_\Xi \cdot (\hat{\Xi}\times\hat{n})}{P_0} \right\rangle \quad \text{are zero.}$$

Hence the precession of the Ξ^- polarization cannot produce an anisotropy in $\hat{\Lambda}\cdot\hat{K}$ or $\hat{\Lambda}\cdot\hat{\Xi}$. From observed distributions of γ and $\theta_{\Xi}^{(c.m.)}$ we estimate the rms angles

$$\left\langle \left[d(\vec{P}_{\Xi}\cdot\hat{\Xi})/P_0 \right]^2 \right\rangle^{1/2} \approx 1.5^\circ$$

$$\left\langle \left[d(\vec{P}_{\Xi}\cdot\widehat{\Xi x n})/P_0 \right]^2 \right\rangle^{1/2} \approx 1.8^\circ \qquad (78)$$

The net effect is a negligible ($\approx$0.05%) decrease in the $\hat{n}$-component of Ξ^- polarization, which is the only component considered in the distribution function [Eq. (35)]. conclude that the precession of Ξ^- polarization vector cannot bias our measurement of Ξ^- decay parameters.

(ii) <u>Precession of Λ polarization</u>.

At t = 0, the instant of Ξ decay, the Λ have direction $\hat{v}(0) = \hat{\Lambda}$ and polarization $\vec{P}(0) = \vec{P}_{\Lambda}$ specified by helicity components $\vec{P}_{\Lambda}\cdot\hat{\Lambda}$, $\vec{P}_{\Lambda}\cdot\hat{x}$, and $\vec{P}_{\Lambda}\cdot\hat{y}$ ($\hat{x}$ and $\hat{y}$ are now defined as in Fig. IV-1). After a time interval $dt = \gamma d\tau$, a Λ initially having a longitudinal polarization $\vec{P}_{\Lambda} = P_0\hat{\Lambda}$ will have acquired transverse polarization components given by

$$d\vec{P}_{\Lambda}\cdot\begin{Bmatrix}\hat{x}\\ \hat{y}\end{Bmatrix} = P_0\, C_1[\hat{H}\times\hat{\Lambda}\cdot\begin{Bmatrix}\hat{x}\\ \hat{y}\end{Bmatrix}]\,\gamma d\tau$$

$$= P_0\, C_1\left\{\frac{\sin\phi_{\Lambda}\cos\phi_{\Xi}^{(c.m.)}}{-\sin\theta_{\Lambda}\sin\phi_{\Xi}^{(c.m.)}+\cos\theta_{\Lambda}\cos\phi_{\Lambda}\cos\phi_{\Xi}^{(c.m.)}}\right\}\gamma d\tau, \qquad (79)$$

delete dashed line(?)

where $(\theta_{\Lambda},\phi_{\Lambda})$, corresponding to (θ,ϕ) of Fig. IV-1, describe the Λ direction in the Ξ rest frame. (Terms proportional

to C_2 vanish for neutral particles.) Similarly, a Λ initially having polarization $P_0\hat{x}$ will have acquired a y-component given by

$$d\hat{P}_\Lambda \cdot \hat{y} = P_0\, C_1\, [\hat{H} \times \hat{x} \cdot \hat{y}]\, \gamma d\tau \qquad (80$$

$$= P_0\, C_1 [-\sin\theta_\Lambda \cos\phi_\Lambda \cos\phi_\Xi^{(c.m.)} - \cos\theta_\Lambda \sin\phi_\Xi^{(c.m.)}]\, \gamma d\tau\ .$$

(With signs reversed represent the precession of x- and y-components onto the Λ-axis, and of the y-component onto the x-axis.) Each of the above expressions averages to zero upon integration over $\phi_\Xi^{(c.m.)}$; were this not the case, the precession described by Eqs. (79) and (80) could result in a biased determination of α_Ξ and/or J_Ξ, and Φ_Ξ, respectively. Averaging each of the expressions over the observed γ and $(\theta_\Lambda, \phi_\Lambda)$ distributions, we estimate the rms angles as

$$\left\langle [d(P_0\hat{\Lambda}) \cdot \hat{x}/P_0]^2 \right\rangle^{1/2} \approx 2.9^\circ;$$

$$\left\langle [d(P_0\hat{\Lambda}) \cdot \hat{y}/P_0]^2 \right\rangle^{1/2} \approx 3.7^\circ; \qquad (81)$$

$$\left\langle [d(P_0\hat{x}) \cdot \hat{y}/P_0]^2 \right\rangle^{1/2} \approx 3.3^\circ.$$

The net effect is a slight uncertainty in the true direction of the Λ polarization vector, which is not of such a nature as to bias our measurement of the Ξ^- decay parameters.

FOOTNOTES AND REFERENCES

* Work performed under the auspices of the U.S. Atomic Energy Commission.

† Present address: CEN-Saclay, B.P. No. 2, Gif-sur-Yvette, France.

‡ Present address: Physics Department, University of Massachusetts, Amherst, Massachusetts.

1. J. Peter Berge, Philippe Eberhard, J. Richard Hubbard, Deane W. Merrill, Janice Button-Shafer, Frank T. Solmitz, and M. Lynn Stevenson, Phys. Rev. 147, 945 (1966).

2. D. Duane Carmony, Gerald M. Pjerrou, Peter E. Schlein, William E. Slater, Donald H. Stork, and Harold K. Ticho, Phys. Rev. Letters 12, 482 (1964); P. E. Schlein, Carmony, Pjerrou, Slater, Stork, and Ticho, Phys. Rev. Letters 11, 167 (1963).

3. G. W. London, R. R. Rau, N. P. Samios, S. S. Yamamoto, M. Goldberg, S. Lichtman, M. Primer, and J. Leitner, Phys. Rev. 143, 1034 (1966).

4. L. Jauneau et al., in Proceedings of the Sienna International Conference on Elementary Particles, Sienna, Italy, 1963 (Societa Italiana di Fisica, Bologna, Italy, 1963), p. 1; and L. Jauneau et al., ibid., p. 4.

5. H. Schneider, Phys. Letters 4, 360 (1963).

6. Janice Button-Shafer and Deane W. Merrill, Spin and Decay Parameters of the Ξ^- Hyperon, UCRL-11884, Jan. 1965.

7. P. Eberhard, J. Button-Shafer, and D. Merrill, Decay Properties of the Ξ^- Hyperon, UCRL-11427, July 1964.

8. J. Richard Hubbard, Properties of the Neutral Cascade Hyperon (Ph.D. thesis), UCRL-11510, April, 1966 (unpublished).

9. Gerald A. Smith, James S. Lindsey, Joseph J. Murray, Janice Button-Shafer, Angela Barbaro-Galtieri, Orin I. Dahl, Philippe Eberhard, William E. Humphrey, George R. Kalbfleisch, Ronald R. Ross, Frank T. Shively, and Robert D. Tripp, Phys. Rev. Letters 13, 61 (1964).

10. Gerald A. Smith, James S. Lindsey, Janice Button-Shafer, and Joseph J. Murray, Phys. Rev. Letters 14, 25 (1965).

11. Janice Button-Shafer, James S. Lindsey, Joseph J. Murray, and Gerald A. Smith, Phys. Rev. 142, 883 (1966).

13. J. Murray, J. Button-Shafer, F. Shively, G. Trilling, J. Kadyk, A. Rittenberg, D. Siegel, J. Lindsey, and D. Merrill, A Separated 2.5 to 2.8 GeV/c K^- Beam at the Bevatron, in Proceedings of the International Conference on High Energy Physics, Dubna, USSR, 1964 (Atomizdat, Moscow, 1966), Vol. II, p. 541; and UCRL-11426, July 1964.

14. Deane W. Merrill, Design of the K-63 Beam Using an Analog Computer, Alvarez Group Physics Memo 519 (Rev.), August 1964; (next page)

12. J. Button-Shafer, G. R. Kalbfleisch, D. H. Miller, J. Kirz, C. G. Wohl, J. R. Hubbard, D. O. Huwe, H. K. Ticho, and D. H. Stork (submitted to Rev. Sci. Instr.)

(14 cont'd)

S. Flatté, S. Chung, L. Hardy, and R. Hess, K-63: Changing the Incident K^- Momentum from 2.7 GeV/c to 2.1 GeV/c, Alvarez Group Physics Memo 524, August 1964.

15. Joseph J. Murray, Glass Cathodes in Vacuum-Insulated High-Voltage Systems, in Proceedings of International Conference on Instrumentation for High-Energy Physics, Berkeley, California, September 1960 (Interscience Publishers, New York, 1961), p. 25.

16. Daniel Siegel, Joseph J. Murray, Alan Rittenberg, and Janice Button-Shafer, Quadrupole Magnet Analysis and Shimmming, Alvarez Physics Memo NFD-518, July 1964.

17. Compelling interest in 1.7 BeV/c K^- (especially by Shafer) prompted ~~xxdxxxigxxxxd~~ realignment of the 2.1 BeV/c beam channel, which yielded good K^- flux at 1.7 BeV/c.

18. Events containing Ξ^- (event-types 12, 72, and 74) were measured exclusively on Franckensteins; events containing Ξ^0 (types 32, 40, and 42) were measured on SMP's as well as Franckensteins.

19. For a description of the standard analysis procedure and computer programs, see A. H. Rosenfeld and W. E. Humphrey, Ann. Rev. Nucl. Sci. 13, 103 (1963).

20. Knowledge of the final state governs only the division of events into arbitrary subsamples (see Table III-2). Inclusion of the ambiguous events can bias

measured values of the Ξ^- polarization but not of the Ξ^- decay parameters α_{Ξ^-} and Φ_{Ξ^-}.

21. Deane W. Merrill, Decay Properties of the Ξ Hyperon and Ξ^* Resonances (Ph.D. Thesis), University of California Radiation Laboratory Report UCRL-16455, Sept., 1966 (unpublished).

22. Gerald A. Smith and James S. Lindsey, Final-State Interaction Involving Hyperons, in Proceedings of the Second Topical Conference on Recently Discovered Resonant Particles, Ohio University, Athens, Ohio, June 1965 (Ohio University Press, Athens, Ohio, 1965) p. 251; and UCRL-16162, June 1965.

23. J. Badier et al., Physics Letters 16, 171 (1965); and J. Badier et al., B = 1, S = -2 States in K^-p Interactions at 3 GeV/c, in Proceedings of the International Conference on High-Energy Physics, Dubna, USSR, 1964 (Atomizdat, Moscow, 1966), Vol. I, p. 593.

24. A. Halsteinslid et al., Preliminary Results on $\Xi^- + K^{0,+} + n(\pi)$ Final States Produced by 3.5 GeV/c K^-, in Proceedings of the Sienna International Conference on Elementary Particles, Sienna, Italy, 1963 (Società Italiana di Fisica, Bologna, Italy, 1963), Vol. I, p. 173.

25. A. H. Rosenfeld, A. Barbaro-Galtieri, W. H. Barkas, P. L. Bastien, J. Kirz, and M. Roos, Data on Elementary Particle and Resonant States, UCRL-8030 (Part I) Rev., August 1965.

26. R. H. Capps, Phys. Rev. 122, 929 (1961).

27. R. Gatto and H. P. Stapp, Phys. Rev. 121, 1553 (1961).

28. N. Byers and S. Fenster, Phys. Rev. Letters 11, 52 (1963), and unpublished appendix of Byers and Fenster, Dept. of Physics, University of California, Los Angeles, May 1963.

29. M. Ademollo and R. Gatto, Phys. Rev. 133, B531 (1964).

30. Janice Button-Shafer, Phys. Rev. 139, B605 (1965).

31. Charles Zemach, Phys. Rev. 140, B109 (1965).

32. S. M. Berman and M. Jacob, Spin and Parity Analysis in Two-Step Decay Processes, Stanford Linear Accelerator Center Report SLAC-43 (Stanford University, Stanford, California, May 1965).

33. J. Button-Shafer, Likelihood Function for Weak Decay of Fermion with Arbitrary Spin, Alvarez Group Physics Memo 533, December 1964.

34. Henry P. Stapp, Relativistic Transformation of Spin Directions, UCRL-8096, December 1957.

35. Consider a momentum four-vector $(\vec{p},E)$ in frame 1, with frame 2 having velocity $\vec{v}$ relative to frame 1. Mathematically, the direct Lorentz transformation corresponds to (i) a rotation to align $\vec{v}$ with the z-axis; (ii) a Lorentz transformation along the z-axis (p_x and p_y are unchanged); (iii) the inverse of the rotation in (i).

36. W. S. C. Williams, An Introduction to Elementary Particles (Academic Press, New York, 1961), pp. 173-174; and Janice Button, Use of the Density Matrix and Scattering Matrix in Calculating Intensities and Polarizations in Some General Types of Interactions, Alvarez Group Physics Memo 337, September 1961.

37. T. D. Lee and C. N. Yang, Phys. Rev. 109, 1755 (1958).

38. R. H. Capps, Ref. 26; N. Byers and S. Fenster, Ref. 28; R. H. Dalitz, "Constraints on the Statistical Tensor," Clarendon Laboratory preprint; P. Minnaert, "Spin Density Matrix Analysis," Ecole Polytechnique preprint; L. Michel, private communication. Only the first two, Refs. 26 and 28, were available at the time of the studies reported here.

39. Our definition of the $\mathcal{D}^{J}_{m_1 m_2}$ functions corresponds to that of Ref. 41.

40. See Ref. 30, Eqs. (3), (11), and (38).

41. M. Jacob and G. C. Wick, Ann. Phys. 7, 404 (1959).

42. This is similar to the distribution I(θ) for a "formation" resonance. See J. Button-Shafer, Phys. Rev. 150, 1308 (1966).

43. Cf. Eq. 24 of Ref. 30. (Zemach in Ref. 31 also presents a similar relation, though he utilizes different language.)

44. John M. Blatt and Victor F. Weisskopf, Theoretical Nuclear Physics (Wiley Press, New York, 1952), p. 361.

45. James W. Cronin and O. E. Overseth, Phys. Rev. 129, 1795 (1963).

46. See Appendix E of Ref. 21.

47. Given N subsamples having $|t_{10}^{actual}| \approx t_{10}^{max}$, we expect half of these, on the average, to yield experimental values $|t_{10}^{obs}| > t_{10}^{max}$, thereby producing a decrease of $\approx N/4$ in $\ln \mathcal{L}$ when the constraint is applied. Our data are consistent with J = 3/2, with $\approx$ 30 of the 47 subsamples having $|t_{10}^{actual}| \approx t_{10}^{max}$.

48. We define the S and P amplitudes as

$$S = |S|\, e^{i\Delta S} = \rho_S e^{i\delta_S}$$

$$P = |P|\, e^{i\Delta P} = \rho_P e^{i\delta_P}$$

where δ_S and δ_P are final-state $\Lambda\pi$ scattering phase shifts. Invariance under T (C) requires that ρ_S and ρ_P be relatively real (imaginary). As no spin-1/2 $\Lambda\pi$ resonances are known in the vicinity of 1320 MeV, δ_S and δ_P are expected to be small.

49. S. B. Treiman, The Weak Interactions, in <u>Dispersion Relations and Elementary Particles</u> (Lectures for Summer School of Theoretical Physics, Les Houches, 1960), edited by C. DeWitt and R. Omnes (Wiley Press, New York, 1960), p. 526.

50. Benjamin Lee, Phys. Rev. Letters <u>12</u>, 83 (1964).

51. See, for example, Murray Gell-Mann, Phys. Rev. Letters <u>12</u>, 155 (1964); Hirotaka Sugawara, Progr. Theoret. Phys. (Kyoto) <u>31</u>, 213 (1964); and Sidney Coleman and S. L. Glashow, Phys. Rev. <u>134</u>, B671 (1964).

52. Roger O. Bangerter, Angela Barbaro-Galtieri, J. Peter Berge, Joseph J. Murray, Frank T. Solmitz, M. Lynn Stevenson, and Robert D. Tripp, Phys. Rev. Letters 17, 495 (1966).

53. M. L. Stevenson, J. P. Berge, J. R. Hubbard, G. R. Kalbfleisch, J. B. Shafer, F. T. Solmitz, S. G. Wojcicki, and P. G. Wohlmut, Phys. Letters 9, 349 (1964); and erratum, Phys. Letters 17, 358 (1965).

54. See N. Cabibbo, p. 29, Proceedings of the XIIIth International Conference on High-Energy Physics, Berkeley, California, September, 1966 (University of California Press, Berkeley, California), and especially Appendix B by J. P. Berge, for world-average results, which include those presented here.

55. D. Berley, S. Hertzbach, R. Kofler, S. Yamamoto, W. Heintzelman, M. Schiff, J. Thompson, and W. Willis, Phys. Rev. Letters 17, 1071 (1966).

56. World-average values are tentative values from a forthcoming compliation by Arthur H. Rosenfeld, Angela Barbaro-Galtieri, Janos Kirz, William J. Podolsky, Matts Roos, William J. Willis, and Charles Wohl, Data on Elementary Particles and Resonant States, UCRL-8030 (Rev.), August 1966.

57. A. Pais, Rev. Mod. Phys. 38, 215 (1966).

58. For a discussion of the statistical treatment (suggested by N. Byers), see Appendix C of Ref. 6.

59. R. H. Dalitz, invited paper "Resonant States and Strong Interactions," Proceedings of the Oxford International Conference on Elementary Particles, (1965).

60. Like the bubble-chamber coordinate system (x_{ch}, y_{ch}, z_{ch}), the systems (x, y, z) and (x', y', z') are left-handed in real space; i.e., $\hat{x}(\hat{x}')$, $\hat{y}(\hat{y}')$, and $\hat{z}(\hat{z}')$ lie roughly along $\hat{z}_{ch}$, $\hat{x}_{ch}$, and $\hat{y}_{ch}$, respectively. For purposes of this discussion we assume the magnetic field to point along $-\hat{z}_{ch}$ (which is not really the case) so that negative particles curve toward $+\hat{x}_{ch}$, as desired.

61. Here $\vec{p}_{\Xi}^{\,(lab)}$ is measured at the Ξ decay vertex.

62. For most events, $\cos\theta_{\Lambda}'^{(\Xi)}$ is more nearly equivalent to $(\hat{\Lambda}\cdot\hat{K})$ than to $(\hat{\Lambda}\cdot\hat{\Xi})$, since $\vec{p}_{\Xi}^{\,(lab)}$ is more nearly parallel to $\hat{K} = \hat{p}_K^{(c.m.)}$ than to $\hat{\Xi} = \hat{p}_{\Xi}^{(c.m.)}$. Nevertheless, due to the forward ($\hat{\Xi}\cdot\hat{K} \approx +1$) peak in the Ξ production distribution, $\cos\theta_{\Lambda}'^{(\Xi)}$ is roughly equivalent to $(\hat{\Lambda}\cdot\hat{\Xi})$ as well as to $(\hat{\Lambda}\cdot\hat{K})$.

63. The observed distribution of $p_{\Xi}^{(lab)}$ extends from 0.5 to 3.0 BeV/c, with a mean value near 1.7 BeV/c. Approximately 80% of the events lie between the representative values 1.0 and 2.4 BeV/c.

64. See Appendix B of Ref. 21.

65. James E. Simmons, Effect of Proton-Proton Scattering on an Initial Longitudinal-Spin Polarization (Ph.D. thesis), UCRL-3625, Jan. 1957. A covariant derivation is given by V. Bargmann, Louis Michel, and V. L. Telegdi, Phys. Rev. Letters 2, 435 (1959).

66. For Ξ^-, ~~Eq.~~ Eq. (70) expresses the rate of precision relative to fixed axes defined at the Ξ^- production vertex, which we have used. Relative to axes rotating with the Ξ^- momentum, the $\hat{H}$-component of $\vec{\omega}(t)$ is $C_1' = C_1 - \omega_{cy}$, where ω_{cy}, the cyclotron frequency, is $-eH/\gamma mc$. For the case of protons, C_1' reduces to the familiar form $\gamma(\mu-1)\omega_{cy}$.

67. M. A. B. Beg and A. Pais, Phys. Rev. 137, B1514 (1965). The experimental value of μ_Λ is -0.73 ± 0.17. [See D. A. Hill and K. K. Li, Phys. Rev. Letters 15, 85 (1965).]

FIGURE CAPTIONS

Fig. II-1. K-63 Beam (top view). S1 and S2 are electrostatic separators; M1, M2, M3, and M4 are bending magnets; Q1, Q2,....Q13 are quadrupoles.

Fig. II-2. K-63 beam profile in (a) vertical plane and (b) horizontal plane. The y-axis (beam direction) is compressed by a factor of 80 relative to x and z, and effects of bending magnets have been ignored.

Fig. II-3. Schematic drawing of first mass slit: (a) ~~seen~~ end ~~on;~~ view; (b) top view of lower jaw. The y-axis (beam direction) is compressed by a factor of 6 relative to x and z. High- and low-momentum K^- (2% above and below the ~~nominal~~ central momentum) are focused at A and B respectively; π^- are focused $\approx$ 1/8" above the K^- image and pass through the uranium upper jaw of the slit.

Fig. IV-1. Diagram of Ξ production and decay via the sequence (A) $K^-+p\rightarrow\Xi+K$; (B) $\Xi\rightarrow\Lambda+\pi$; (C) $\Lambda\rightarrow p+\pi$. The Ξ production angle Θ is defined in the production c.m. frame (A); angles θ and ϕ describe Λ decay in Ξ rest frame (B); Λ polarization is described with reference to axes x and y, illustrated in the blowup of system (B). Momentum four-vectors of Ξ, Λ, and p are obtained from measured lab momenta

via successive Lorentz transformations through frames (A), (B), and (C).

Fig. V-1. Correlation between α_Λ and α_{Ξ^-} for combined K-72 and K-63 sample. With no external information on α_Λ, the best fit to the data yields $\alpha_\Lambda = 0.698 \pm 0.069$, $\alpha_{\Xi^-} = -0.381 \pm 0.045$ (standard-deviation ellipse centered at A). With an additional factor of $\exp[-(1/2)(\alpha_\Lambda - 0.62)^2/(0.07)^2]$ in the likelihood, the best fit yields $\alpha_\Lambda = 0.657 \pm 0.047$, $\alpha_{\Xi^-} = -0.394 \pm 0.041$ (ellipse centered at B). **Projections shown represent quoted α_Λ and α_Ξ values with errors.**

Fig. V-2. Distributions of $(\hat{p}\cdot\hat{\Lambda})$ for 3431 Ξ^- events. (See Table III-1.) K-72 events are shaded. The theoretical curve is proportional to $1 + \alpha_\Lambda \alpha_\Xi (\hat{p}\cdot\hat{\Lambda})$, where $\alpha_\Lambda \alpha_{\Xi^-} = -0.28$.

Fig. V-3. Decay distributions of 3431 Ξ^- events (K-72 and K-63 data combined). The theoretical curves correspond to the best fit with α_Λ free, namely $\alpha_\Lambda = 0.698 \pm 0.069$, $\alpha_{\Xi^-} = -0.381 \pm 0.045$, $\Phi_{\Xi^-} = 10.0^\circ \pm 8.9^\circ$, $\langle P_\Xi \rangle = 0.26 \pm 0.04$. Most of the (very weak) evidence for Φ_{Ξ^-} or $\beta_{\Xi^-} > 0$ comes from 179 Ξ^-K^+ events at 2.45 and 2.55 BeV/c, having $\langle P_{\Xi^-} \rangle = 0.90 \pm 0.19$ and $\sum_{i=1}^{179} (\hat{p}\cdot\hat{y})_i = 12.3 \pm 7.7$ and yielding $\Phi_{\Xi^-} = 30^\circ \pm 18^\circ$ when fitted separately. All other subsamples have smaller average polariz-

ations and yield values of Φ_{Ξ^-} consistent with zero.

Fig. V-4. Dependence of $w = \ln\mathcal{L}$ upon assumed spin factor $(2J+1)$, for 3278-event Ξ^- sample. The decrease of 3.02 in $\ln\mathcal{L}$ indicates discrimination against the $J = 3/2$ hypothesis by 2.45 standard deviations. The additional decrease of 7.03, due to violation of the $J = 3/2$ density matrix constraint, is not statistically significant.

Fig. V-5. Measured values of $X = \Delta\ln\mathcal{L}$ for (a) 15 Ξ subsamples; and (b) 75 Monte Carlo samples generated assuming $J = 1/2$, $\alpha_\Lambda = 0.62$, $\alpha_\Xi = -0.40$, $\Phi_\Xi = 0$, $t_{10} = 0$. The curve shown in (b) represents $\bar{X} = 0$, $\sigma_{X_{u.c.}} = 0.27$.

Fig. V-6. Measured values of $X = \Delta\ln\mathcal{L}$ for (a) 75 Monte Carlo samples generated assuming $J = 1/2$, $\alpha_\Lambda = 0.62$, $\alpha_\Xi = -0.40$, $\Phi_\Xi = 0$, $t_{10} = t_{10}^{max} = 0.57$; and (b) 75 Monte Carlo samples having $J = 3/2$, $\alpha_\Lambda = 0.62$, $\alpha_\Xi = -0.40$, $\Phi_\Xi = 0$, $t_{10} = t_{10}^{max} = 0.43$. Curves shown represent (a) $\bar{X} = 1.66$, $\alpha_\Xi = 1.93$; (b) $\bar{X} = -0.67$, $\sigma_{X_{u.c.}} = 1.07$.

Fig. V-7. Scatter plot and projections for $\Xi\pi$ mass-squared vs. $\Xi\pi\pi$ mass-squared for 164 $\Xi K\pi\pi$ events from the K-63 run.

Fig. V-8. Scatter plot of events having $\Xi\pi\pi$ and $\Xi\pi_2$

masses corresponding to the $\Xi^*(1817)$ and $\Xi^*(1530)$. For removal of events with $K\pi_1$ mass $\approx K^*$ mass.

Fig. V-9. Two decay-angle distributions for events which qualify for $\Xi^*(1817) \rightarrow \Xi^*(1530) \rightarrow \Xi$. In plot (a) any significant amount of $|\cos\theta|^2$ contribution would demand that the spin of the $\Xi^*(1817)$ be 3/2 or higher.

Fig. VI-1. Comparison of decay-parameter results from K-72 and K-63 data with those from previous experiments. (See Table VI-1.)

Fig. VI-2. Representations of the Lee SU_3 triangle (for Ξ, Λ, and Σ decay amplitudes) and the $|\Delta I| = 1/2$ triangle (for Σ decay amplitudes). Experimental results used are new world averages which include the results of this report. (See Table VI-2.)

Fig. VI-3. Values of $X = \Delta\ell n\chi$ vs. $|t_{10}(J=\frac{1}{2})|$ for 45 Ξ^- subsamples and 7 Ξ^0 subsamples. Dashed curves represent the expected range of X ($\bar{X} \pm \sigma_X$) assuming J = 1/2 and J = 3/2, as a function of $|t_{10}^{(1/2)}|$. The solid curve represents the expected distribution in $|t_{10}^{(1/2)}|$ (due to the measurement errors alone) if all subsamples have zero polarization. Points (a), (b), and (c) designate $\langle(\delta t_{10})^2\rangle^{1/2}$, $\langle t_{10}\rangle$ from $\langle t_{10}^2 - (\delta t_{10})^2\rangle^{1/2}$, and $\langle t_{10}^2\rangle^{1/2}$.

Fig. A-1. Distributions in $\hat{\Lambda}\cdot\hat{K}$ and $\hat{\Lambda}\cdot\hat{\Xi}^-$ for the Ξ^- events of Table III-2. (Directions defined in the Ξ rest frame.)

Fig. A-2. Scatter plot (and projection) in ϕ_Ξ and $\cos\theta_\Xi$ ~~θ_Ξ~~ production parameters for the Ξ^- events of Table III-1.

Fig. A-3. Scatter plot (and projection) in decay angles describing the Λ direction in the Ξ rest frame, for the Ξ^- events of Table III-1.

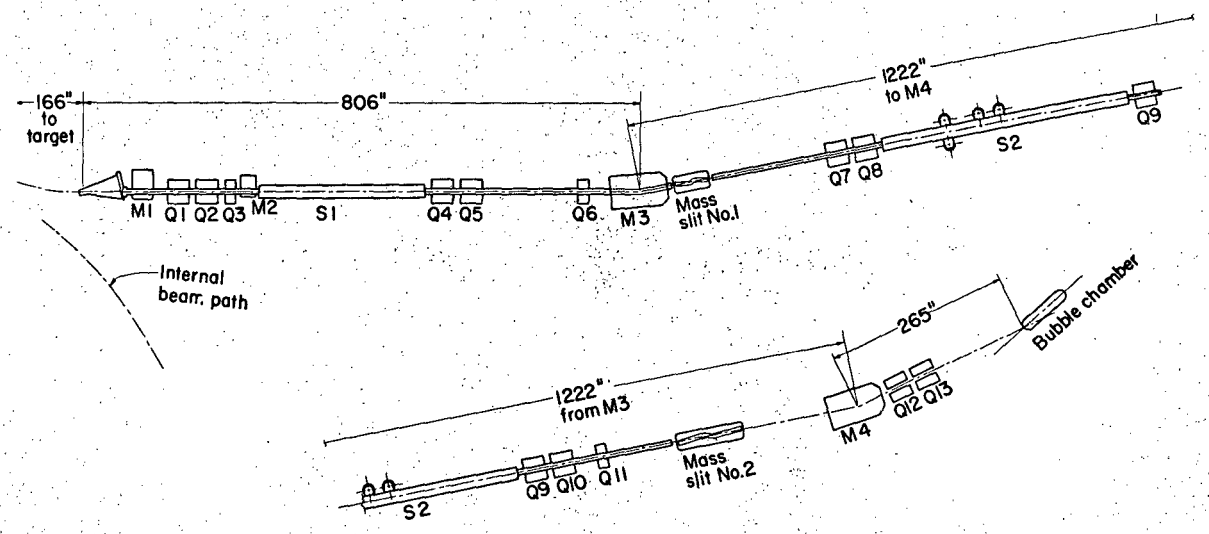

MU-36827

Fig. II-1

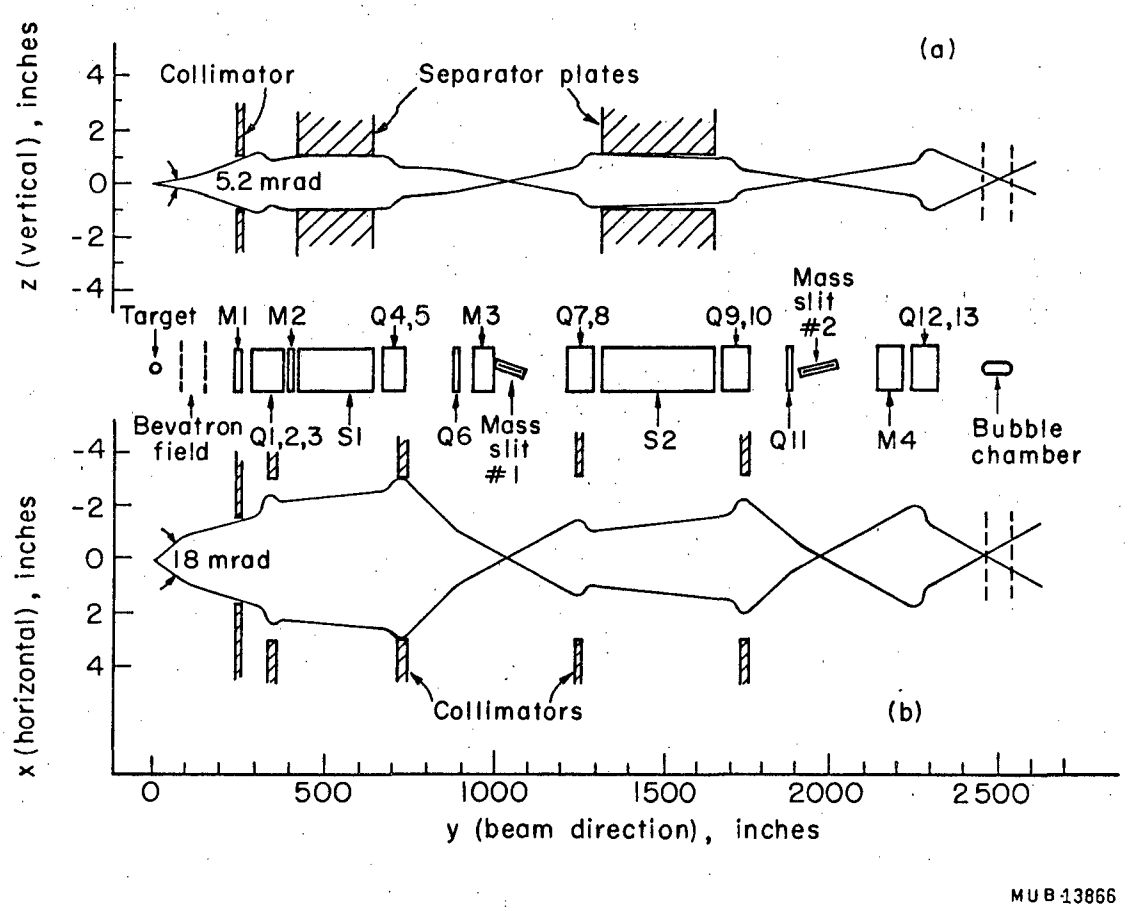
(a)
Collimator
Separator plates
5.2 mrad
z (vertical), inches
4
2
0
-2
-4
Target
M1
M2
Q4,5
M3
Q7,8
Q9,10
Mass slit #2
Q12,13
Bevatron field
Q1,2,3
S1
Q6
Mass slit #1
S2
Q11
M4
Bubble chamber
18 mrad
Collimators
(b)
x (horizontal), inches
0
500
1000
1500
2000
2500
y (beam direction), inches
MUB-13866

Fig. II-2

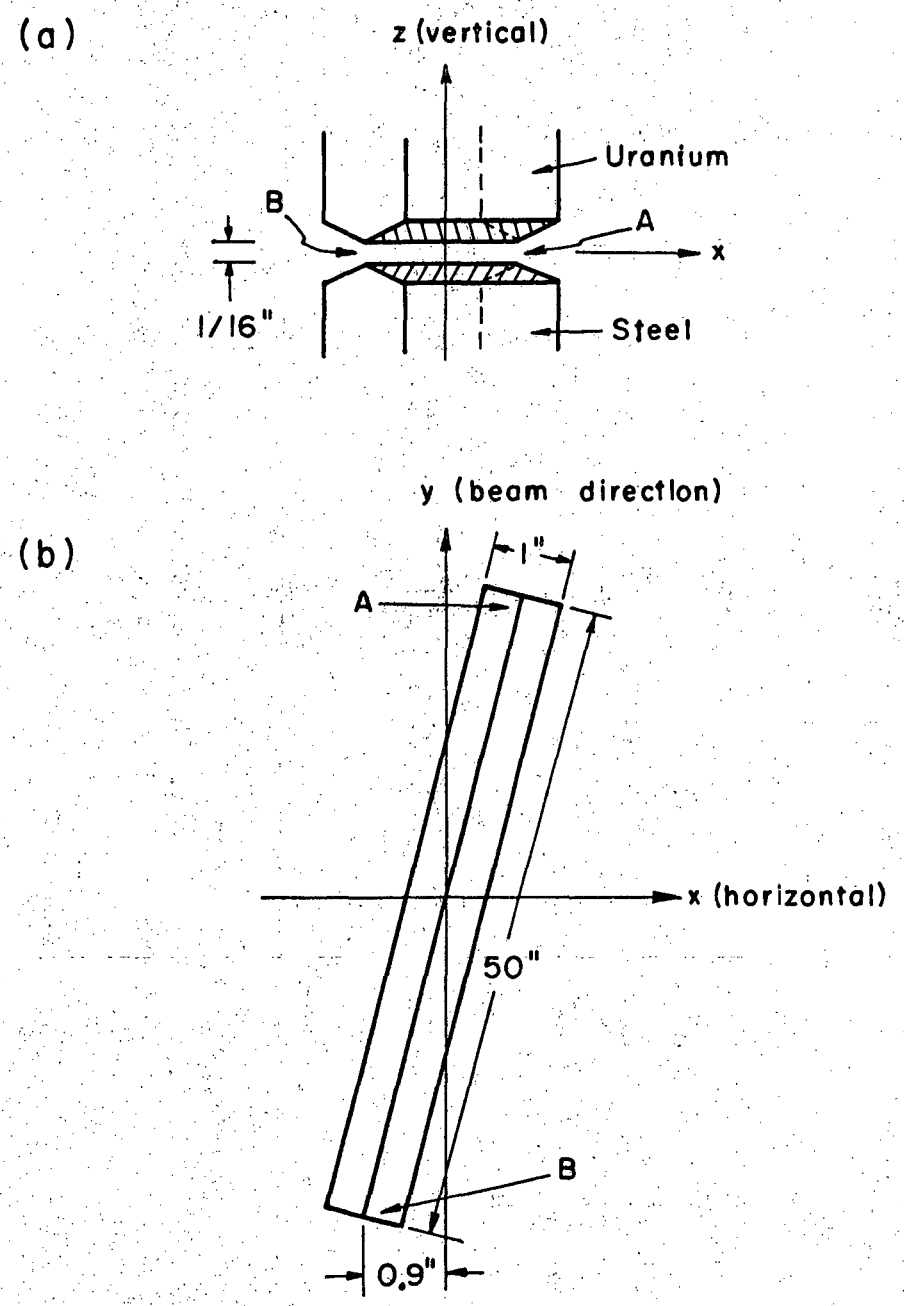
(a)
z (vertical)
Uranium
B
A
x
1/16"
Steel
(b)
y (beam direction)
1"
A
x (horizontal)
50"
B
0.9"
MUB-13867

Fig. II-3

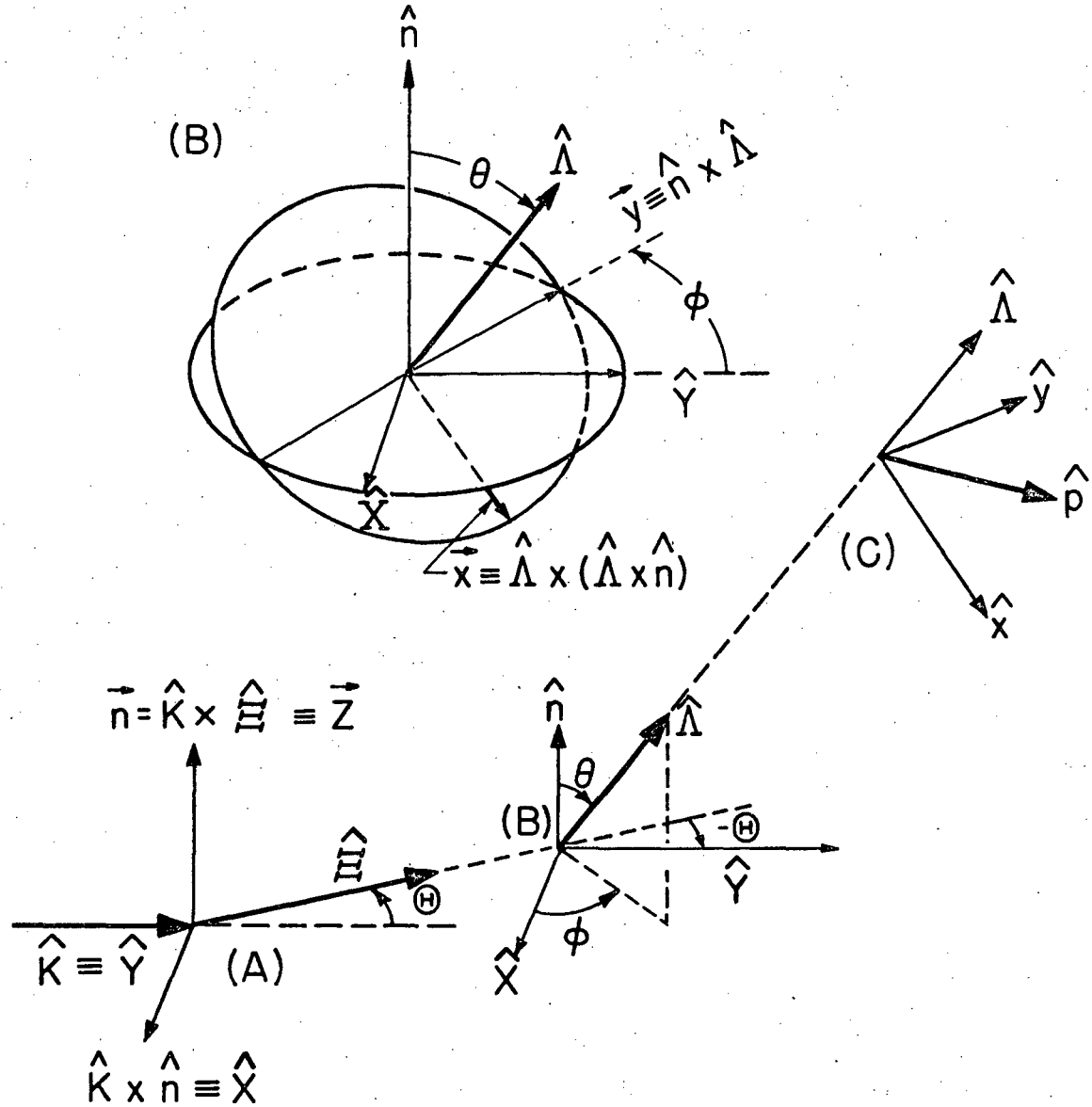

MUB-5077-A

Fig. IV-1

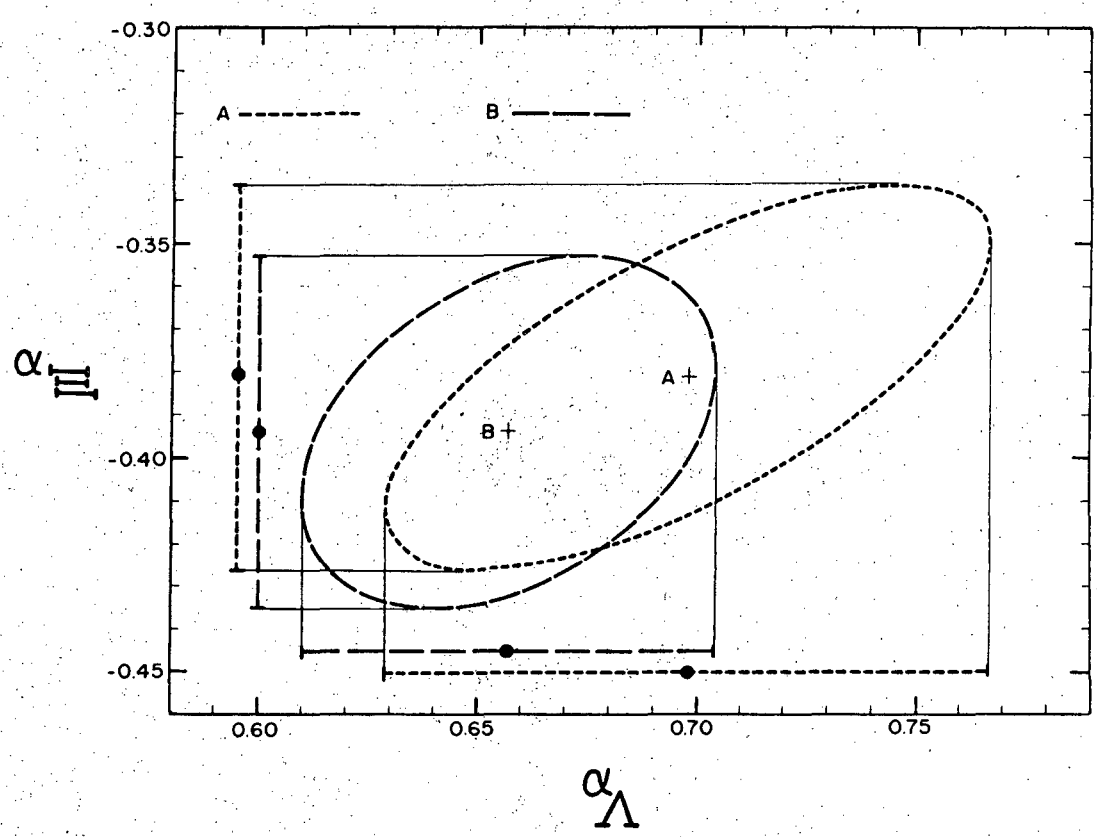

XBL 677-4262

Fig. V-1

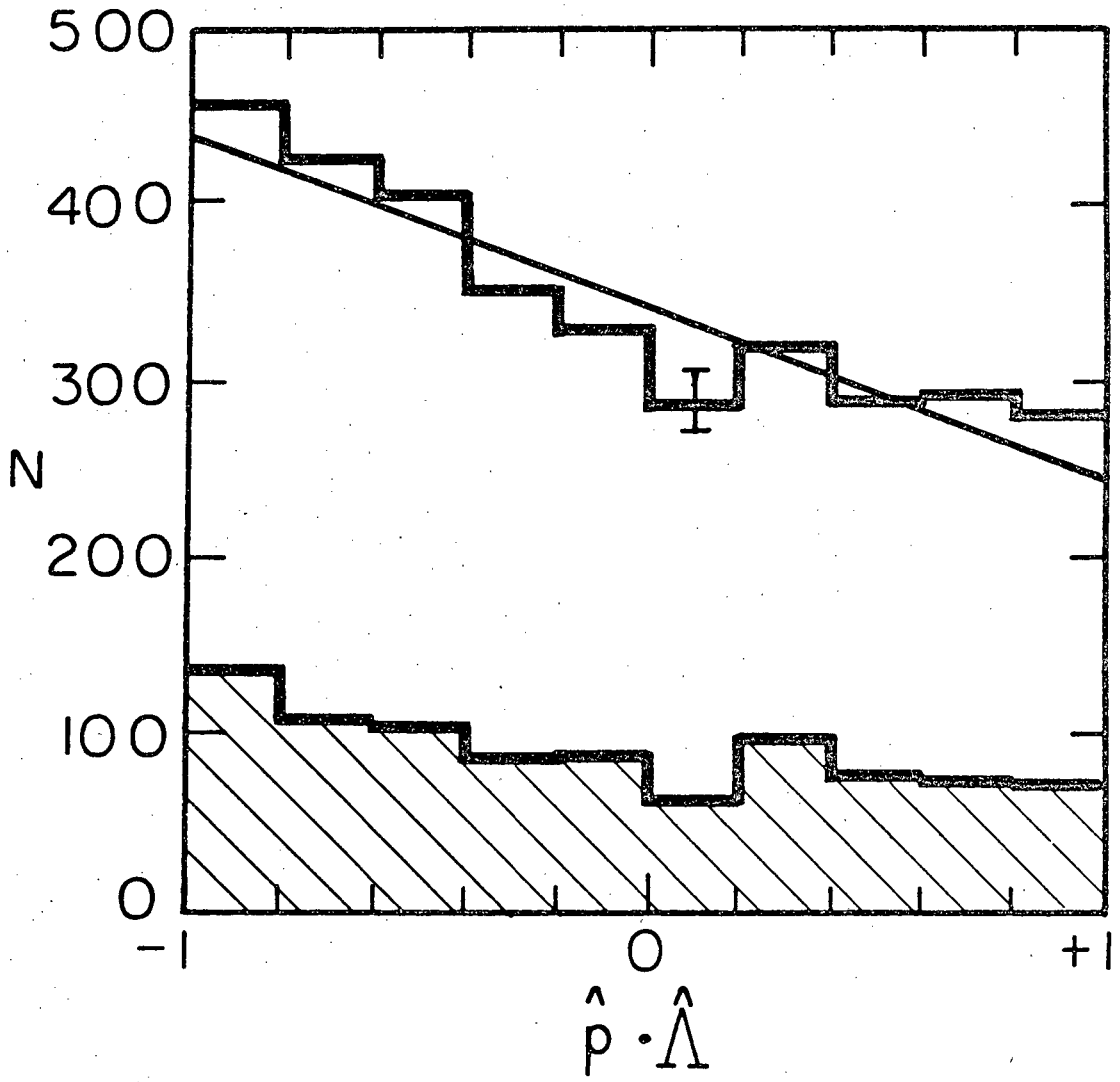

XBL 677-4263

Fig. V-2

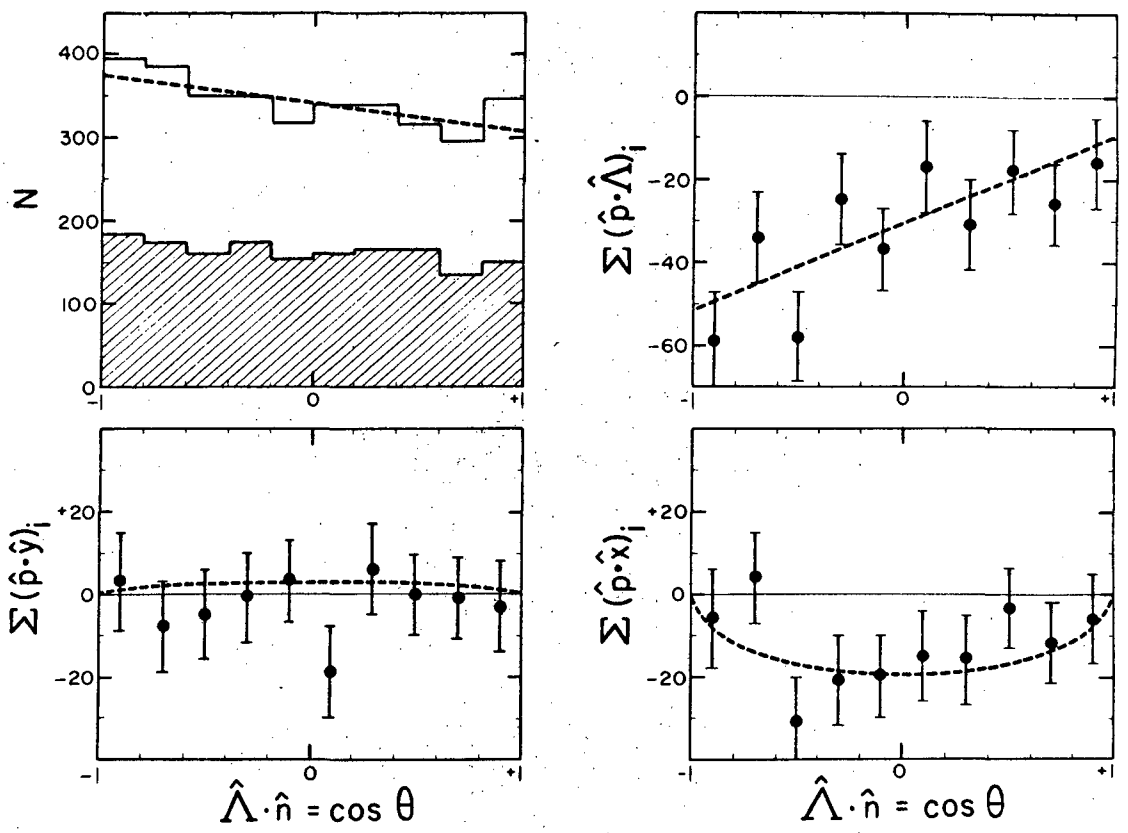

XBL 677-4264

Fig. V-3

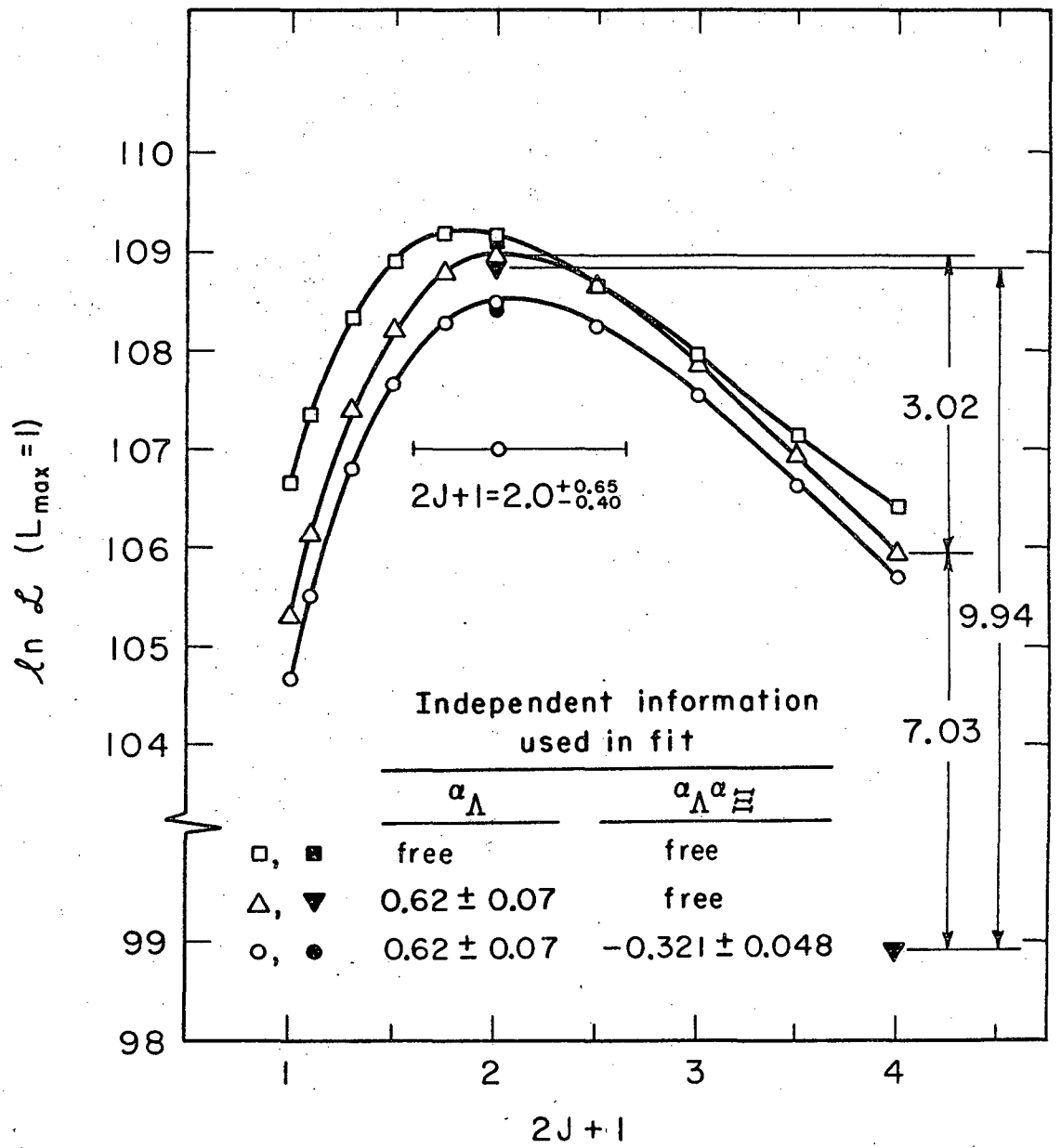

MU-36800

Fig. V-4

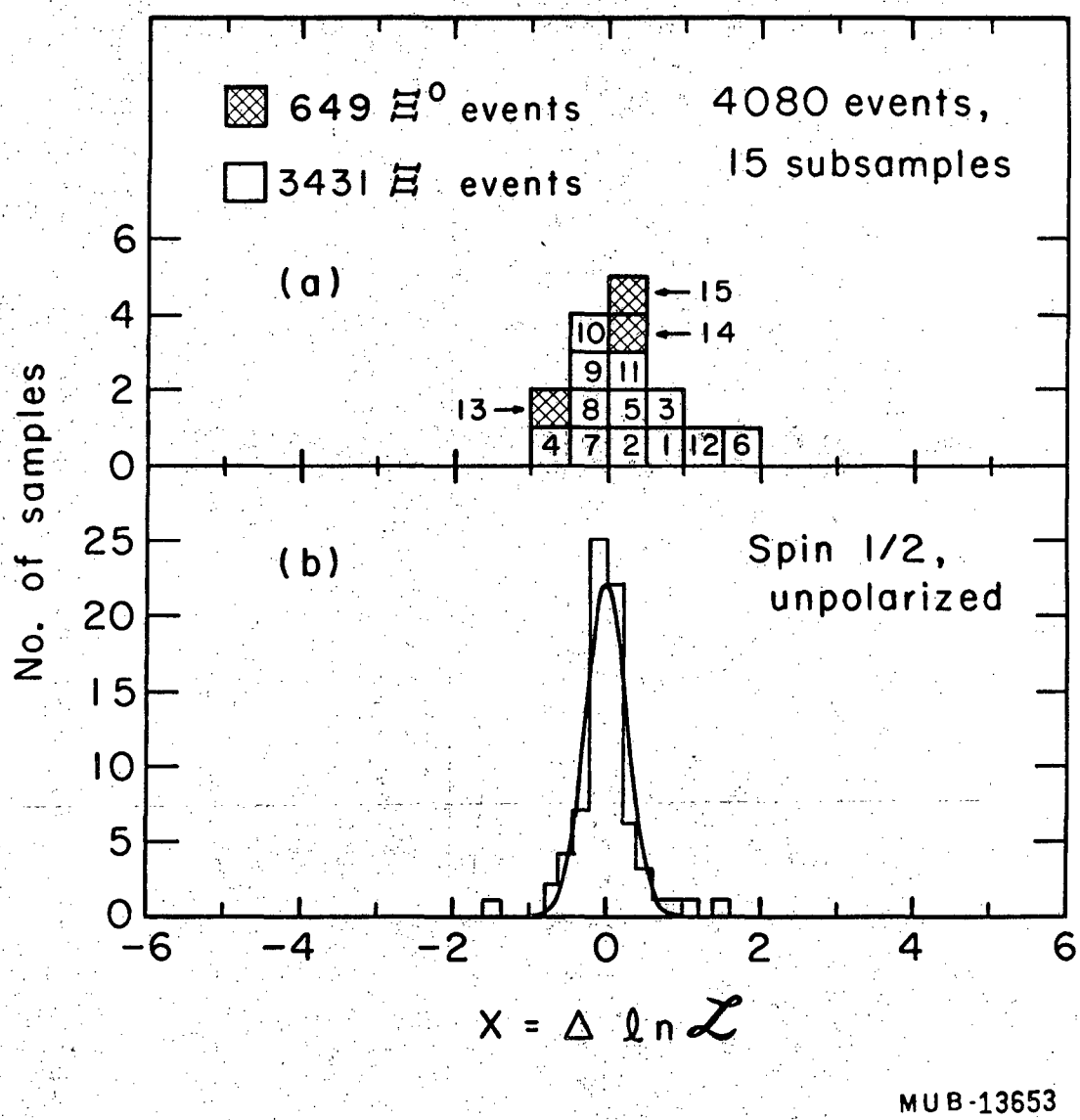
649 Ξ⁰ events
3431 Ξ events
4080 events,
15 subsamples
(a)
(b)
Spin 1/2,
unpolarized
No. of samples
X = Δ ln ℒ
MUB-13653

Fig. V-5

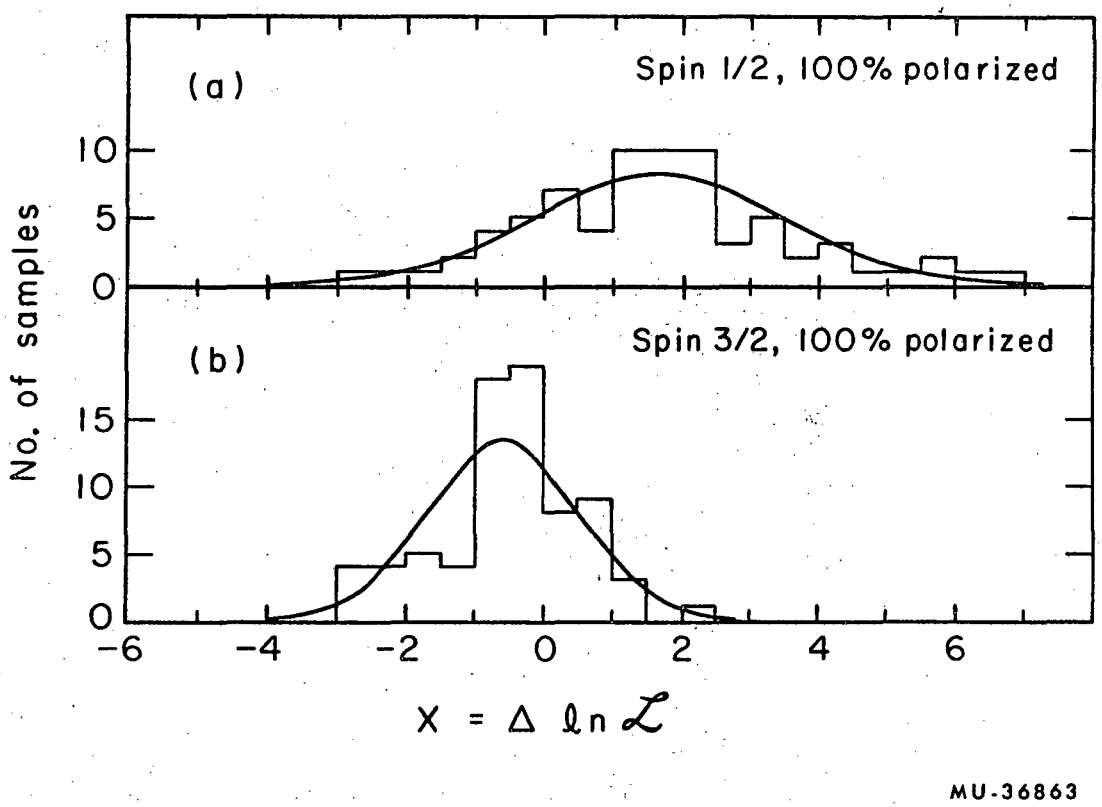

MU-36863

Fig. V-6

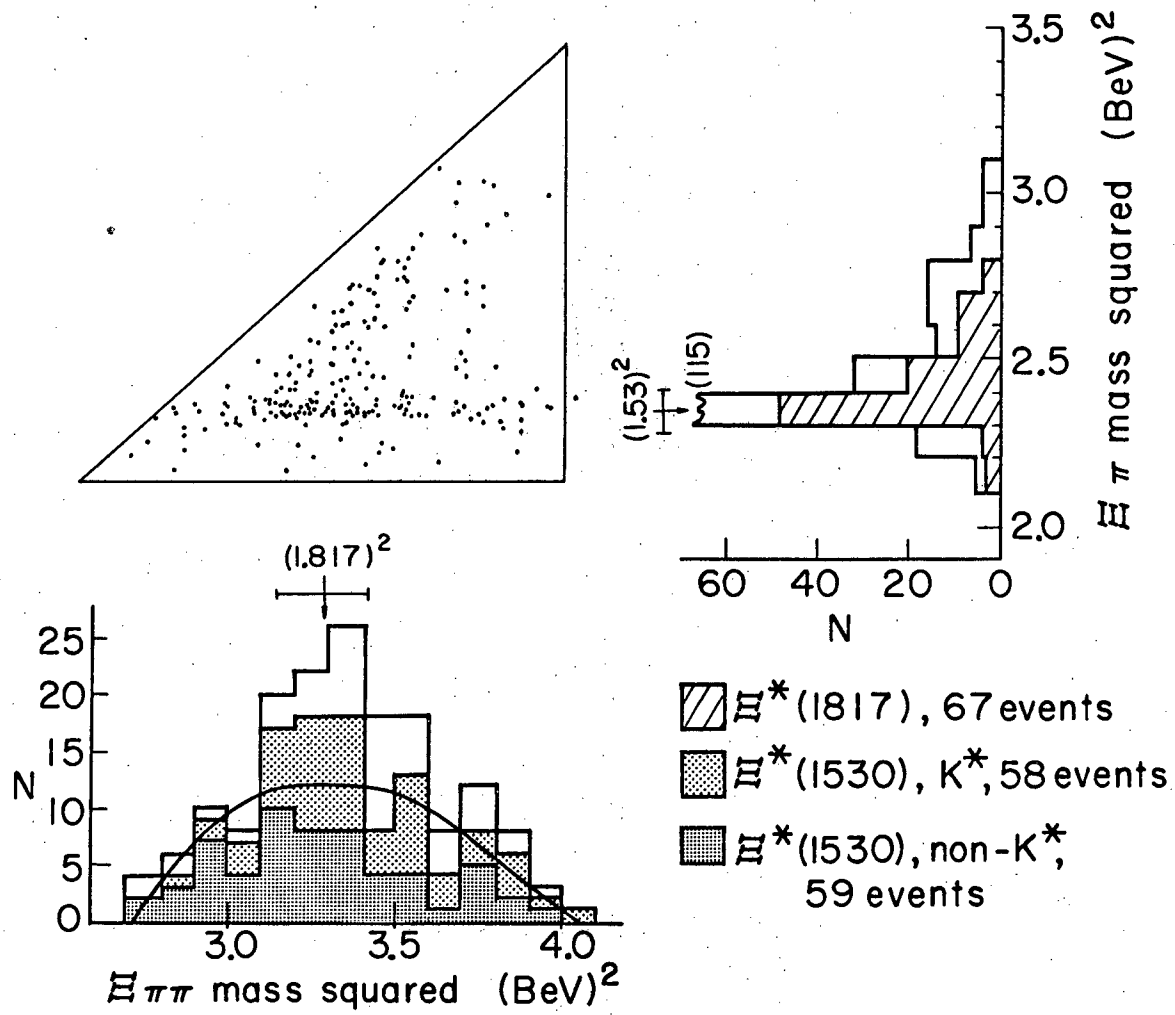

MUB-13657

Fig. V-7

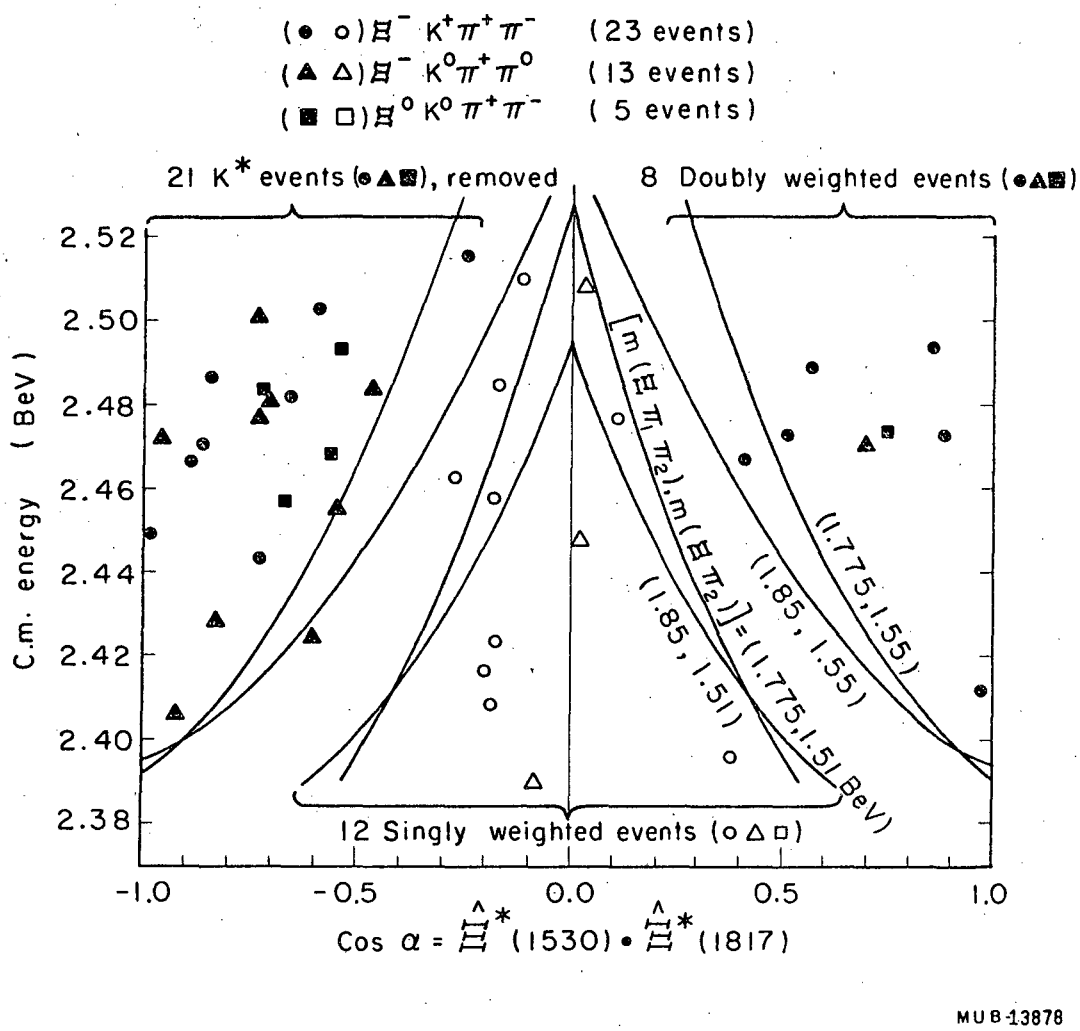
(● ○) Ξ⁻ K⁺π⁺π⁻ (23 events)
(▲ △) Ξ⁻ K⁰π⁺π⁰ (13 events)
(■ □) Ξ⁰ K⁰ π⁺π⁻ (5 events)
21 K* events (●▲■), removed
8 Doubly weighted events (●▲■)
12 Singly weighted events (○ △ □)
[m(Ξ π₁ π₂), m(Ξ π₂)] = (1.775, 1.51 BeV)
(1.85, 1.51)
(1.85, 1.55)
(1.775, 1.55)
C.m. energy (BeV)
2.52
2.50
2.48
2.46
2.44
2.42
2.40
2.38
-1.0
-0.5
0.0
0.5
1.0
Cos α = Ξ̂* (1530) • Ξ̂* (1817)
MUB-13878

Fig. V-8

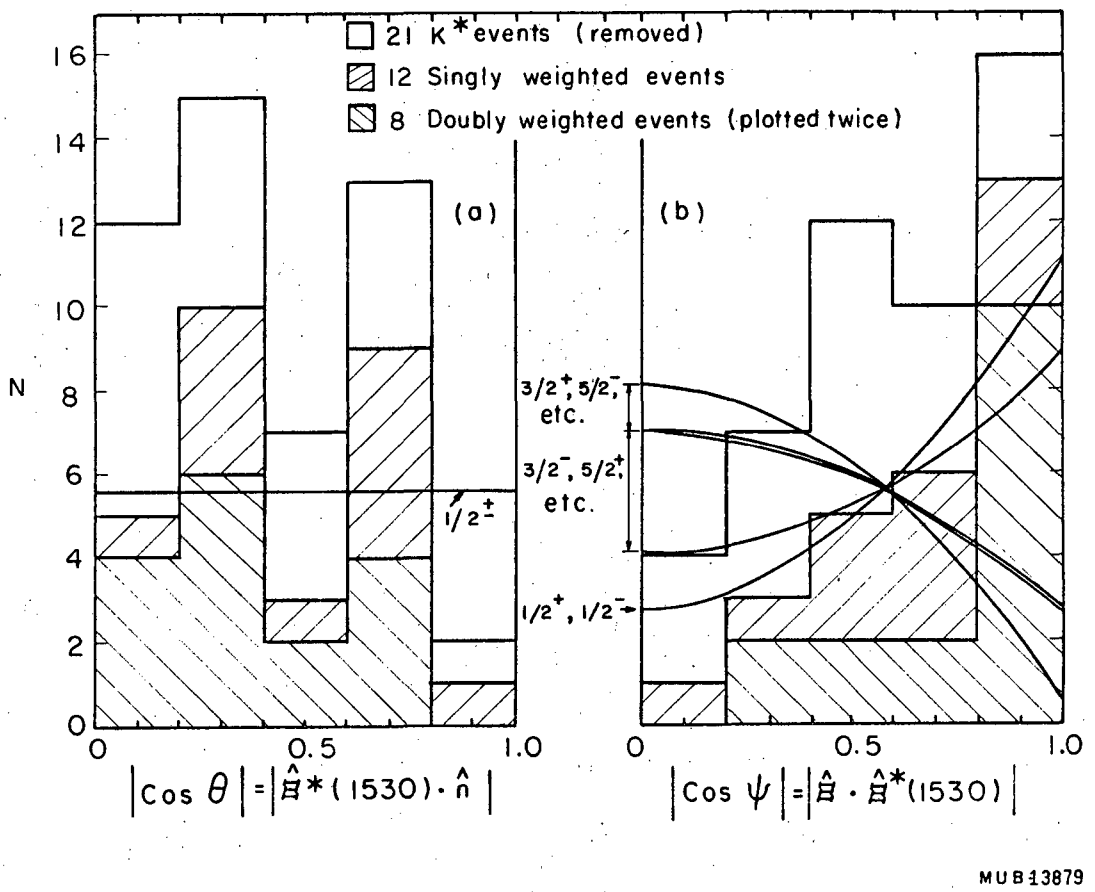
21 K* events (removed)
12 Singly weighted events
8 Doubly weighted events (plotted twice)
(a)
(b)
N
16
14
12
10
8
6
4
2
0
0
0.5
1.0
1/2±
3/2+, 5/2,
etc.
3/2−, 5/2+,
etc.
1/2+, 1/2−
|Cos θ| = |Ĥ*(1530)·n̂|
|Cos ψ| = |Ĥ·Ĥ*(1530)|
MUB 13879

Fig. V-9

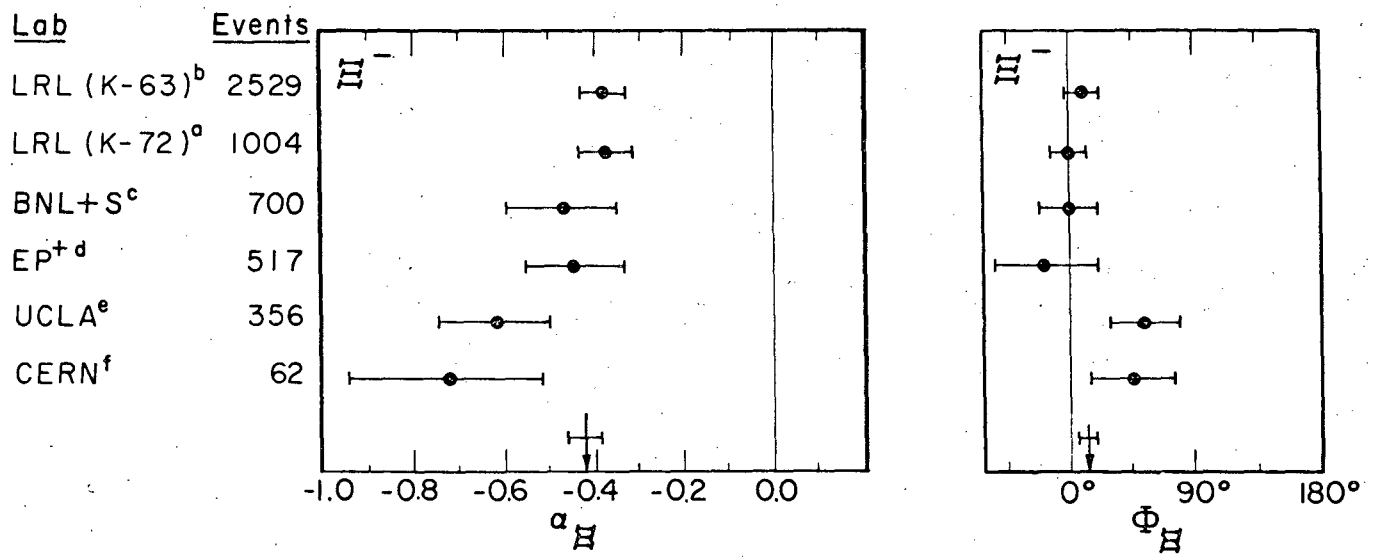

MUB-12253

Fig. VI-1

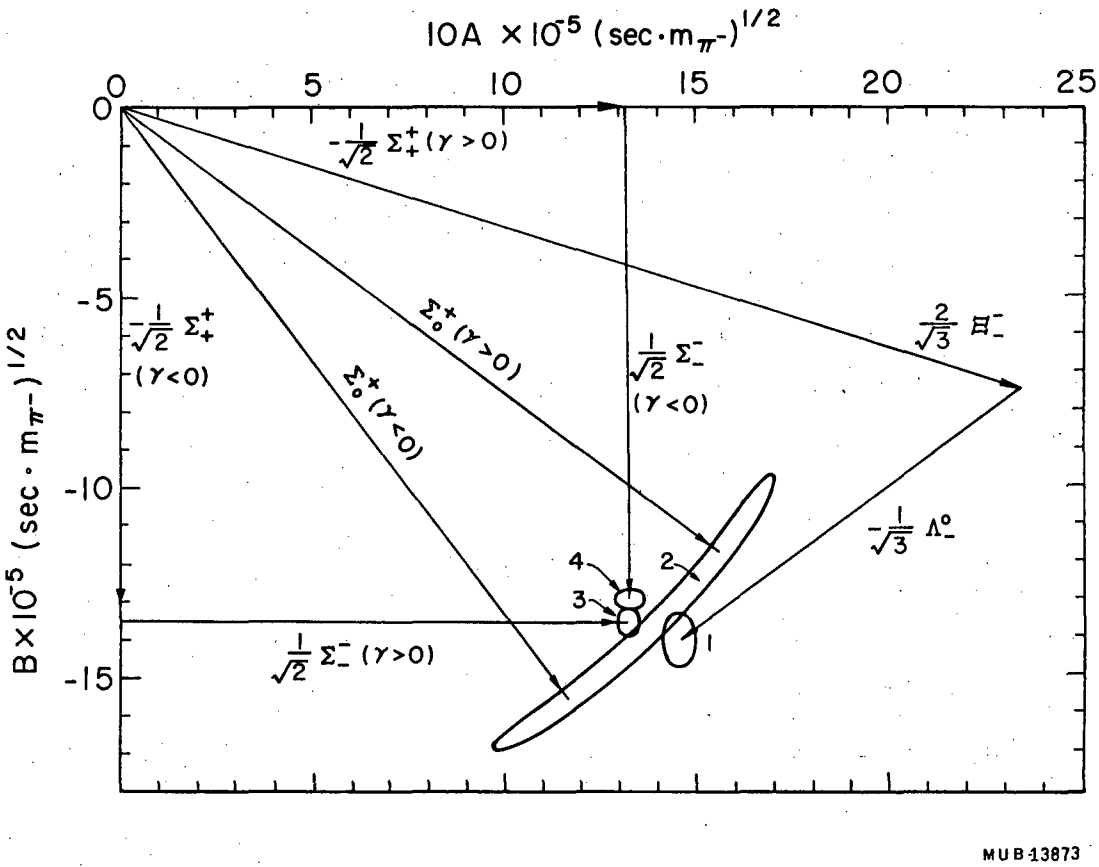
10A × 10⁻⁵ (sec·m_π-)^1/2
0
5
10
15
20
25
0
-5
-10
-15
B × 10⁻⁵ (sec · m_π-)^1/2
-1/√2 Σ+ (γ > 0)
-1/√2 Σ+ (γ<0)
Σ0+ (γ>0)
Σ0+ (γ<0)
1/√2 Σ- (γ<0)
2/√3 Ξ-
-1/√3 Λ0
1/√2 Σ- (γ>0)
1
2
3
4
MUB-13873

Fig. VI-2

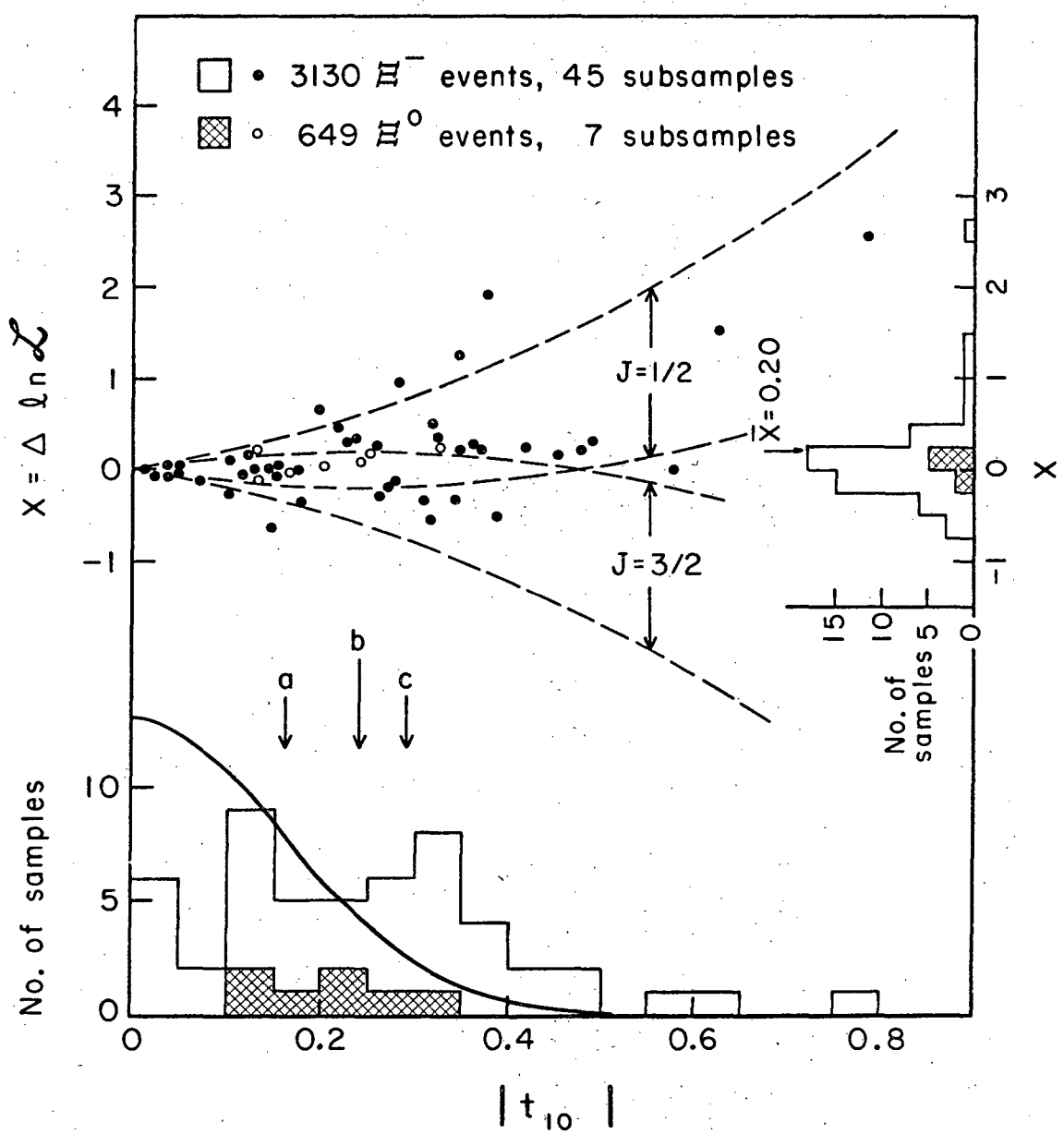

MU-36866

Fig. VI-3

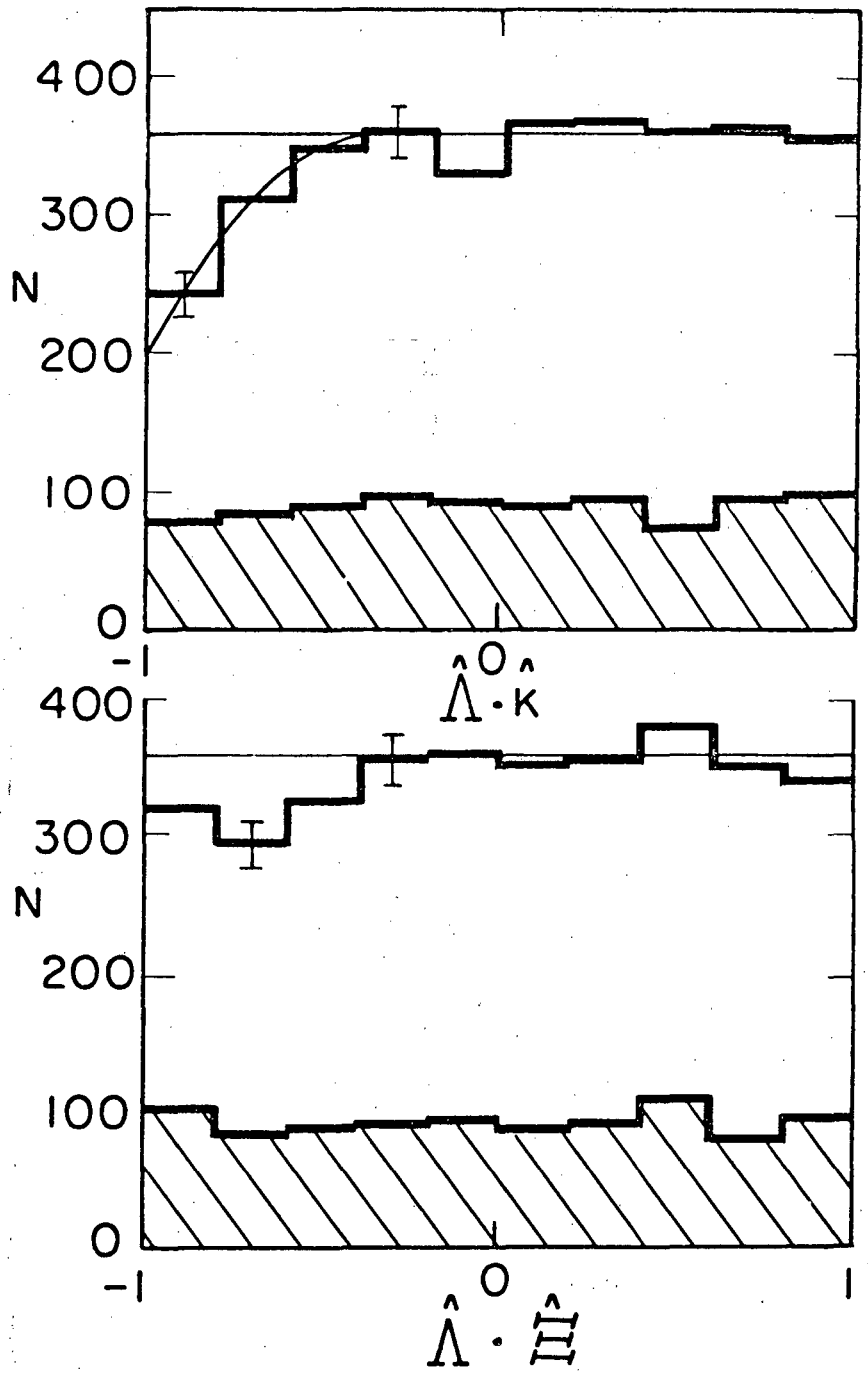

XBL 677-4261

Fig. A-1

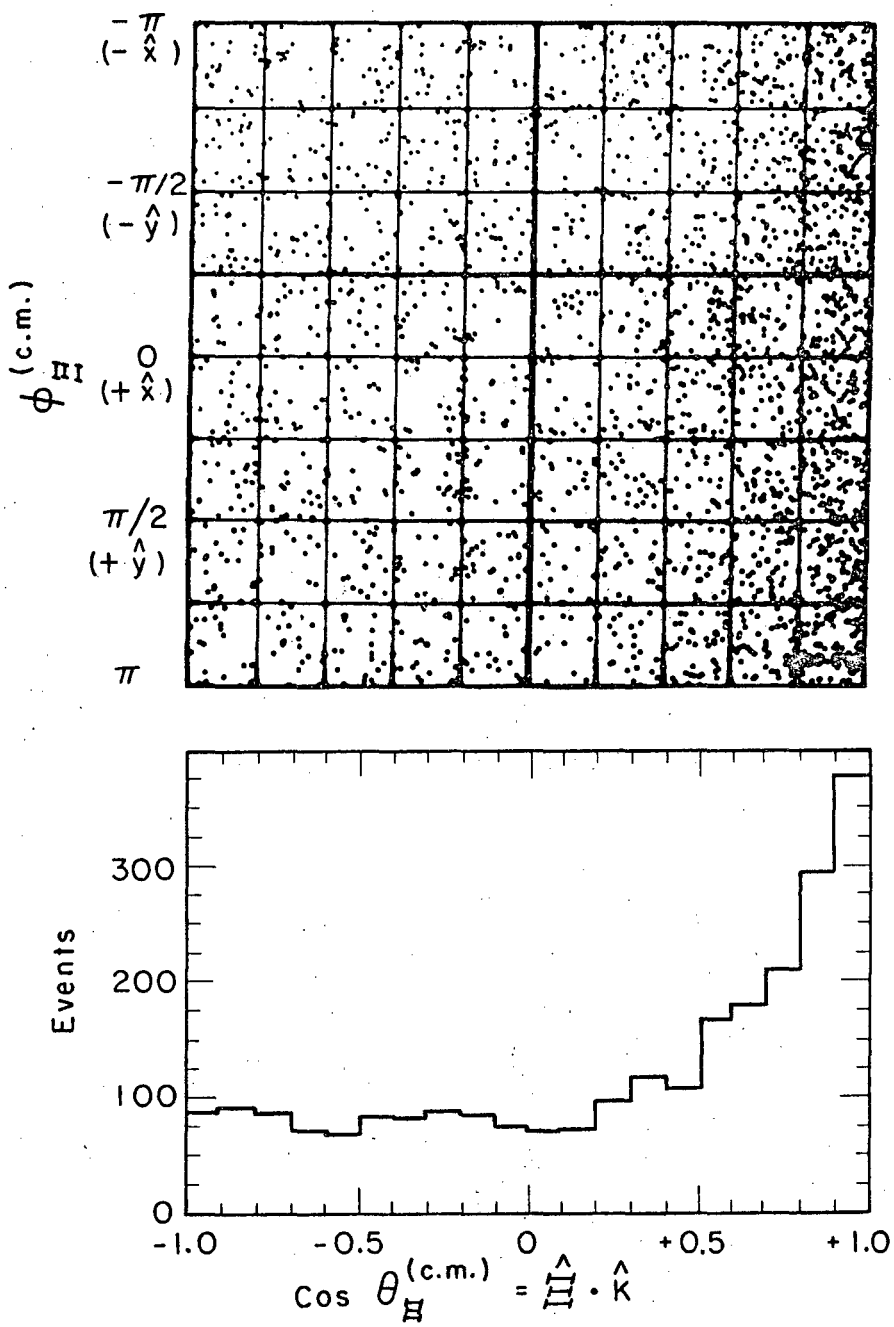
$-\pi$
$(-\hat{x})$
$-\pi/2$
$(-\hat{y})$
$\phi_{\Xi I}^{(c.m.)}$
0
$(+\hat{x})$
$\pi/2$
$(+\hat{y})$
π
Events
300
200
100
0
-1.0
-0.5
0
+0.5
+1.0
$\cos\theta_{\Xi}^{(c.m.)} = \hat{\Xi} \cdot \hat{K}$
MUB-13881

Fig. A-2

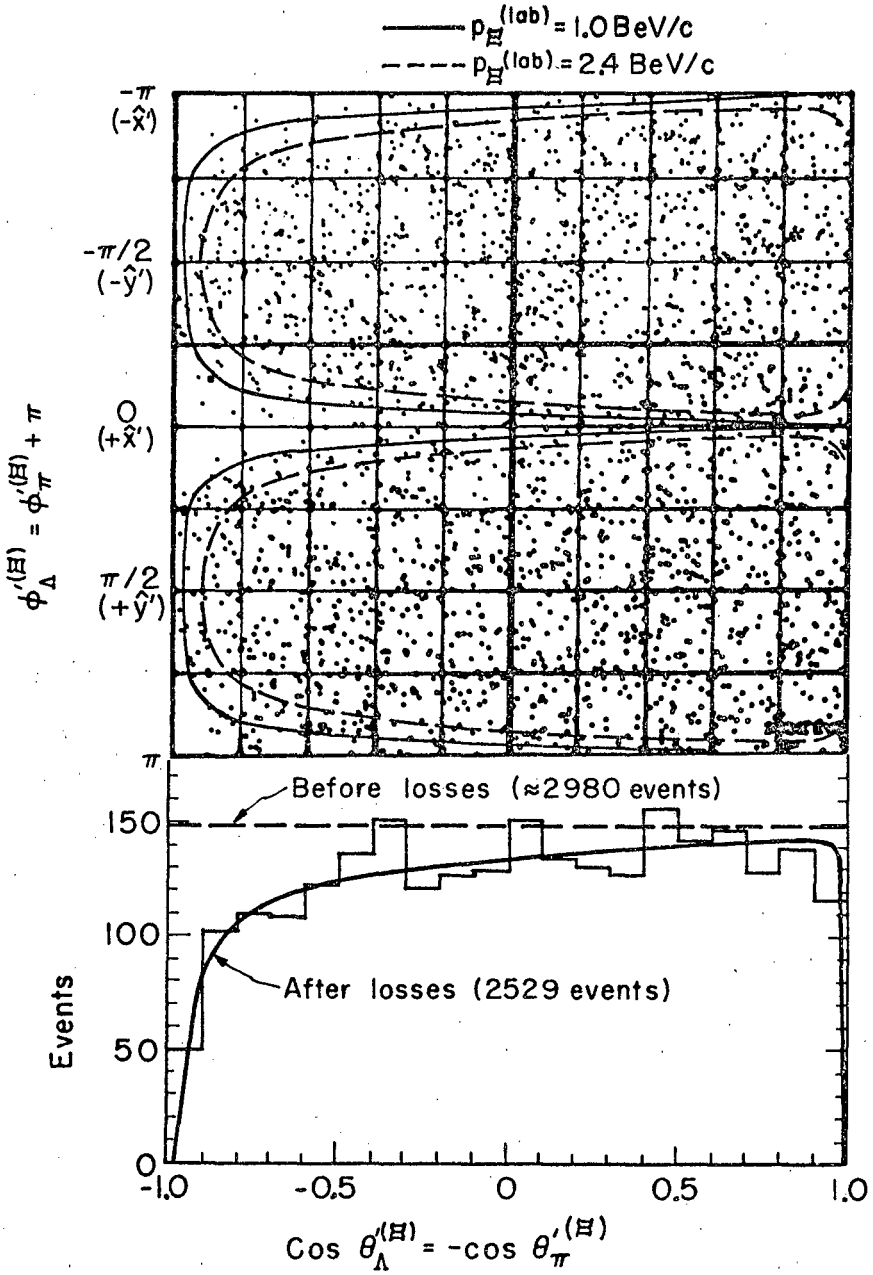

MUB-13882

Fig. A-3

This report was prepared as an account of Government sponsored work. Neither the United States, nor the Commission, nor any person acting on behalf of the Commission:

A. Makes any warranty or representation, expressed or implied, with respect to the accuracy, completeness, or usefulness of the information contained in this report, or that the use of any information, apparatus, method, or process disclosed in this report may not infringe privately owned rights; or

B. Assumes any liabilities with respect to the use of, or for damages resulting from the use of any information, apparatus, method, or process disclosed in this report.

As used in the above, "person acting on behalf of the Commission" includes any employee or contractor of the Commission, or employee of such contractor, to the extent that such employee or contractor of the Commission, or employee of such contractor prepares, disseminates, or provides access to, any information pursuant to his employment or contract with the Commission, or his employment with such contractor.